The Thesis Committee for Scott Alan Grimes
Certifies that this is the approved version of the following thesis:

Novel Phosphonium and Ammonium Ionic Liquids for Green Applications

APPROVED BY
SUPERVISING COMMITTEE:

Supervisor:

Alan H. Cowley

Richard A. Jones

Novel Phosphonium and Ammonium Ionic Liquids for Green Applications

by

Scott Alan Grimes, B.S. CH.

Thesis

Presented to the Faculty of the Graduate School of

The University of Texas at Austin

in Partial Fulfillment

of the Requirements

for the Degree of

Master of Arts

The University of Texas at Austin

May 2014

Dedication

To my parents, whose excessive pride may now be justified, and to Jack, Charity, and Fawn, who serve as a constant reminder of what is truly valuable in life.

Acknowledgements

I'd first like to thank my advisor, Dr. Alan Cowley, for giving me the room and independence to succeed (and not succeed) on my own terms. His dedication to his craft constantly inspires a sense of persistence and patience that is needed to survive this process. More importantly, though, he is a good man who cares about his students, both personally and professionally.

It has been very gratifying to work with Dr. Allen Bard on the electrodeposition project. Despite winning multiple national and international awards, he is still humble and kind and his outlook and expertise actually made me enjoy electrochemistry. I would especially like to thank his post-doc, Dr. Sungki Cho, who performed much of the electrochemisty on our silicon deposition project.

In my teaching career, I'd like to thank Dr. Stacy Sparks for all the experience she has imparted and the trust she has laid upon me. It has been a pleasure working with you to introduce hundreds of students to the joys of chemistry.

To my friends in the Cowley group, Kal, Clint, Rachel, Sarah, Kate, Dan, and Owen: an "acknowledgement" is entirely insufficient to describe what I owe you. Knowing you, laughing with you, and watching you succeed and be happy are worth every moment I spent at UT. More than anything, I've always wanted to help you achieve your dreams. I'd especially like to thank Sarah and Kate, who were my partners through CEC conferences, qualifiers, surprise 4th year talks and other day-to-day problems. I hope I've served you well.

Although I can't list off every person in the inorganic division who I want to thank personally, I would be amiss to not mention Lauren Avery Mitchell and Jordan

Dinser. They have been great friends to me over the years and I wish them all the goodness they deserve.

Abstract

Novel Phosphonium and Ammonium Ionic Liquids for Green Applications

Scott Alan Grimes, M.A.

The University of Texas at Austin, 2014

Supervisor: Alan H. Cowley

New phosphonium and ammonium ionic liquids were prepared for use in two green applications. Ionic liquids are generating considerable current interest as media for electrochemical processes such as electrodeposition, which can be used to create thin films of a variety of compounds. For the first time, silicon deposition has been achieved in the phosphonium ionic liquid triethyl(2-methoxyethyl)phosphonium bis(trifluoromethylsulfonyl)amide (P201-TFSI). Subsequently, silicon has been deposited from a wide variety of precursors in order to optimize the thickness and morphology of the deposited films. The silicon films electrodeposited in the phosphonium ionic liquid show marked differences from those deposited in organic solvents, imidizolium and pyrrolidinium based ionic liquids.

Phosphonium and ammonium ionic liquids were also investigated for use in carbon dioxide capture. Task-specific ionic liquids have shown great promise as agents for the physisorption and chemisorption of CO_2 from combustion gas streams. Efforts to synthesize new task specific ionic liquids with multiple amine functionalities for CO_2

capture are reported. Four different reaction pathways were explored for the synthesis of these materials. While this goal was not achieved in this work, task-specific phosphonium and ammonium ionic liquids offer the promise of opening up new areas in ionic liquid research.

Table of Contents

List of Tables

List of Figures

List of Schemes

PHOSPHONIUM IONIC LIQUIDS

Ionic liquids are an emerging class of materials with a growing number of applications. Conventionally, ionic liquids are defined as ionic compounds with a melting point below 100 ℃ thus differentiating them from liquid phase ionic salts such as NaCl (m.p. 801 ℃) which are usually termed, "molten salts." Most ionic liquids are created from cations of group V alkyl organic compounds such as ammonium, pyrrolidinium, piperidinium, and phosphonium in addition to N-heterocyclic aromatics such as imidizolium and pyridinium. These cations are most often paired with halide or highly fluorinated anions such as tetrafluoroborate (BF_4), and hexafluorophosphate (PF_6). In general, all ionic liquids share some common properties. Foremost among these is the low vapor pressure (approximately 10^{-10} Pa) exhibited at room temperature by the vast majority of ionic liquids. This particular characteristic has spurred a significant amount of research into green applications of ionic liquids as replacements for traditional organic solvents. Other desirable properties common in ionic liquids include high thermal stability, low flammability, intrinsic electrical conductivity, and the ability to solvate a wide range of organic and inorganic compounds.

The hallmark characteristic of ionic liquids as a class, and the principal motivator behind the research in such compounds, relates to their tunability toward desired properties or purposes. By means of the structural variation of both cation and anion, the physical, chemical, or electrochemical properties can be altered to more closely fit the parameters desired for a particular application. While a significant amount of work has been focused on nitrogen-based cations, there has been considerably less attention on phosphonium ionic liquids (PILs).

Chapter 1: Design and Synthesis of Novel Phosphonium Ionic Liquids for the Electrodeposition of Silicon

INTRODUCTION

Intrinsically, ionic liquids exhibit some amount of electrical conductivity. This fact, in conjunction with the high electrochemical stability that is a characteristic of many ILs, makes them attractive as replacements for the typical organic solvent/electrolyte combinations employed in most electrochemical studies. In this respect, phosphonium ionic liquids show promise since previous studies have shown them to possess greater electrochemical stability than their ammonium counterparts while still retaining comparable conductivities. In addition to electrochemical stability, other key properties for media include high conductivity of electrical current, lower viscosity for higher mass diffusion rates, and in some cases, thermal stability. In ionic liquids, these properties are inexorably linked to the structure and electronic behavior of the ion pair.

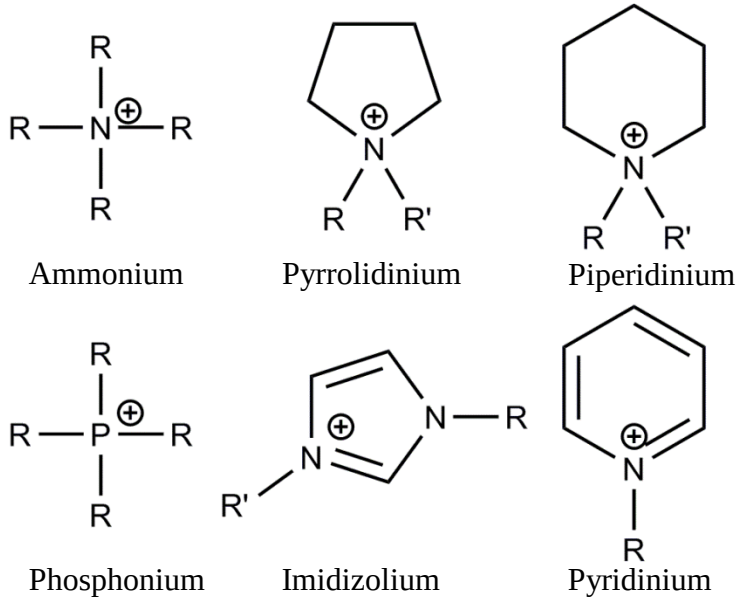

Figure 1.1: Structures of common cations used in ionic liquids.

While general trends in the structure-property relationship have been found in nitrogen-based ionic liquids, there is considerably less work specific to phosphoniums. Nevertheless, the conclusions from such works seem to indicate that phosphoniums follow the same trends as their nitrogen-based counterparts. These trends can be separated into two general categories: electronics which affect the lattice energies of the ionic pair, and sterics which affect the structural packing efficiencies of the molecules.

Electronic considerations are typically the most dominant and obvious effects that influence the behavior of ionic liquids. ILs have significantly lower lattice enthalpies than metal-nonmetal type ionic salts that populate the majority of small ionic compounds. This low lattice enthalpy is due to, in part, greater electron density on the cationic center and less density on the anionic center. In most ionic liquids, this causes a change in anion to often result in a more drastic change in physical properties as compared to a change in cation. While the earliest ionic liquids used "hard" halide or tetrachloroaluminate anions, more recent results show that highly fluorinated or resonance-delocalized anions produce superior ionic liquids. Fluorinated anions such as tetrafluoroborate (BF_4), and hexafluorophosphate (PF_6) have been used extensively and have spurred development of new highly fluorinated ions like $[B(Ar^F)_4]^-$ (Ar^F = -C_6H_3-3,5-CF_3), alcoxyaluminates $[Al(OC(CF_3))_4]^-$ and perfluoroalkylphosphates (FAP) $[PF_3(C_2F_5)_3]^-$ (Figure 1.2).[1–3]

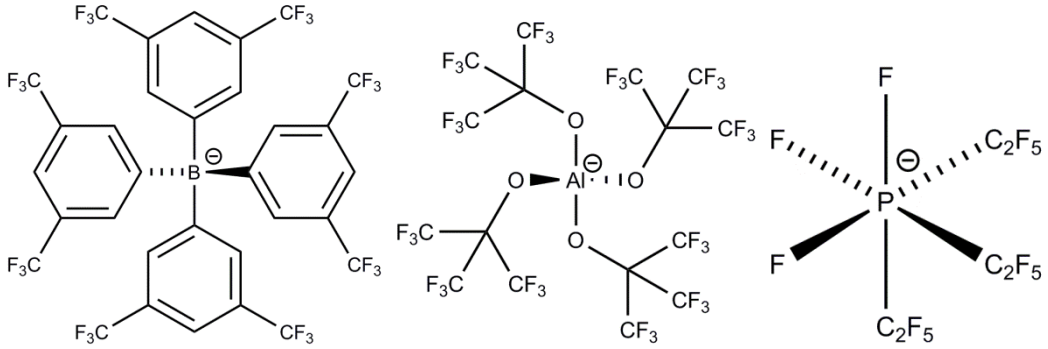

Figure 1.2: Structures of the $[B(Ar^F)_4]^-$, alcoxyaluminate and FAP ions, respectively.

The principle behind this design relies on the ability of the highly electronegative fluorinated groups to draw excess electron density away from the anionic center. The second approach employs anions with a high degree of delocalization that is achieved through resonance. Anions, such as dicyanamide $[N(CN)_2]^-$ and bis(trifluoromethylsufonyl)amide (TFSI) $[N(SO_2CF_3)_2]^-$ (Figure 1.3) have been shown to result in ionic liquids with favorable physical properties.[4]

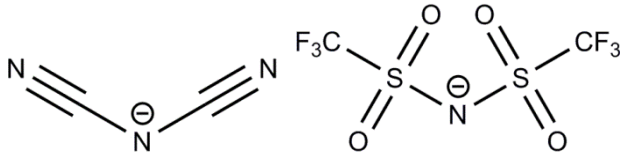

Figure 1.3: Structures of the $[N(CN)_2]^-$ and [TFSI] ions, respectively.

In the case of cations, there are fewer variations available to affect the electron density of the positive center. Alkyl substituents are the most electron donating, while any sp^2 hybridized substituents cause decreased performance. Since most atoms and functional groups tend to be more electron withdrawing than carbon, the vast majority of ionic liquids found in literature use only alkyl substituents. The use of effects resonance in cations is limited yet important. Only N-heterocyclic aromatic cations such as imidizolium and pyridinium use resonance delocalized charges; nevertheless these represent some of the most popular cations in literature due to their excellent physical properties and ease of use. In addition to inductive and resonance effects, small changes can be seen by the use of bigger, electronically softer atoms as the cationic center. This trend can be confirmed by comparing ammonium and phosphonium ionic liquids, where the latter show slightly superior properties than the former.[5]

The second important consideration needed in designing successful ionic liquids relates to the effect of sterics on the efficiency of the molecular crystal packing.

Variations in size, shape, symmetry and flexibility can disrupt crystal packing and lead to liquids with more favorable melting points and viscosities. Chief among these variables is the size and volume of the ions constituting the ionic liquid. Larger ions disrupt packing to a greater extent than smaller ions. However, due to an increased amount of Van der Waals forces, larger ions also tend towards increased viscosity in the resulting ionic liquids. As an example, tributyloctylphosphonium [TFSI] shows a two-fold increase in viscosity in comparison with the smaller triethyloctyl analogue, and is itself almost two-fold less viscous than the larger trihexyltetradecyl analogue.[6,7] Additionally, the shapes of the ions, or the substituents thereon, also play a role in the crystal packing. Tri-*n*-butylmethylphosphonium TFSI melts at 16 ℃ while tri-*i*-butylmethylphosphonium TFSI has a melting point of 52 ℃.[6,8] This increase in melting point indicates an inverse behavior as compared to trends seen in normal aliphatic alkanes.[9] Finally, it should be noted that symmetry and conformational flexibility also play minor roles in ionic liquid physical properties. It is known that molecules with higher symmetry tend to have greater entropy in the solid state than less symmetric molecules, thus making symmetry favorable for crystallization.[10] Finally, the conformational flexibility of the substituents also contributes, as more rigid functional groups tend toward higher crystallinity. Even in flexible alkyl chains, it has been demonstrated that the substitution of an oxygen atom for a carbon can result in a marked decrease in viscosity.[11]

Overall, the design of a successful ionic liquid depends on a balance between steric and electronic factors. Often, gains made in one area, such as lower melting point, are lost in another, such as higher viscosity. While there have been several efforts to create a theoretical framework for the design of ionic liquids,[12–14] the sheer number and variety of ionic liquids has caused investigators to rely more on the empirical results from their subset of interest.

Silicon Electrodeposition

Due to problems such as global warming, resource depletion and instabilities in the cost and availability of crude oil, there is an increasing demand for alternative energy sources that are capable of producing clean energy by avoiding the emission of carbon dioxide. One approach to achieving this goal is by further development of photovoltaic devices that are capable of efficient conversion of solar energy into electricity. There have been several different avenues explored in regard to this goal, including dye-sensitized solar cells,[15] quantum dots,[16] organic polymers,[17] metal oxides,[18,19] and other inorganic systems.[20–22] In terms of conversion efficiency, bulk crystalline silicon is the most prominent among these approaches, exhibiting efficiencies on the order of 25%.[23]Unfortunately, the high temperatures that are required to produce bulk silicon (ca. 1000 °C) in the widely used Siemens and Czochralski processes,[24,25] in conjunction with the rigorous purity demands render bulk silicon very costly. In lieu of this, amorphous and nanocrystalline silicon thin films can be produced under less demanding conditions yet still afford useful efficiencies on the order of 10%.[26,27] However, the latter process is expensive. For example, the deposition of thin films of 300 μm thick silicon accounts for almost 50% of the cost of fabricating a typical photovoltaic device.[28] In order to address this problem, a variety of techniques have been developed for the creation of films with higher efficiencies and lower costs. One of the earliest and most frequently used techniques is chemical vapor deposition (CVD) of silane precursors at moderately high temperatures (ca. 500 °C).[28] Several types of CVD reactors have been utilized for the deposition of these thin films, such as plasma enhanced CVD and ultra-high vacuum CVD. While the foregoing methods represent a significant improvement over the more costly processes that are necessary for the preparation of bulk crystalline silicon, the most

desirable processes would be those that occur close to ambient temperatures and pressures.

Electrodeposition uses current to reduce cationic materials to neutral species deposited on a cathode. The electrodeposition of transition metals, often termed electroplating, has been widely used for approximately 150 years in many industrial applications such as zinc anti-corrosion coatings. These electroplating techniques almost always occur in aqueous solution where the potentials for metal reduction are well within the restrictive electrochemical range of water (roughly 1.6 V, shifted by pH). However, main group, alkali, and alkali earth metal elements often require potentials beyond the reach of water and often react negatively with it. Accordingly, the most common solvents for these systems are large-window organic compounds such as acetonitrile (approx. -2.5 to 2.5 V), DCM (approx. -1.8 to 1.8 V), or THF (approx. -3 to 1.5 V) in combination with an organic electrolyte such as tetrabutylammonium [PF_6].[29] This has lead to the successful deposition of many main group elements such as aluminum,[30] carbon nanomaterials,[31] and germanium.[32]

In 1981 Agrawal and Austin reported the successful deposition of amorphous silicon up to 1 μm in thickness in THF solution.[33] This study established some of the most common trends in silicon electrodeposition. Silicon halides have been used for three primary reasons: the large electronegativity difference between silicon and Cl/Br/I results in lower potentials needed for the reduction of silicon (IV) to neutral silicon, the ultra-high purities of SiX_4 easily achieved through simple distillation, and the availability of these halides which are already used on the multi-ton scale for the thermal production of electronics grade silicon. More recently, Fukunaka et al.[34] explored silicon deposition from propylene carbonate while Munisamy et al.[35] utilized acetonitrile as the solvent. In 2012 Bechelany et al. extended this approach to dichloromethane and observed several

morphological differences between solvents.[36] Problems commonly encountered in silicon deposition attempts include the high potential needed for the four-electron reduction, usually found around -2.5 V vs. Pt quasi-reference electrode, and facile oxidation of the deposits upon exposure to air.

Unfortunately, organic solvents also have some drawbacks, such as volatility, flammability, and sometimes limited potential windows. In this respect, ionic liquids may be an ideal substitute for traditional organic solvents. Users of organic solvents must consider the volatility of a substance and its effect on solution concentration, the environment, and the thermal limit. In contrast, ionic liquids have little to no vapor pressure and are often thermally stable in excess of 300 ℃, at which point they most typically decompose in lieu of vaporizing. Additionally, with judicious choice of ion pairs, ionic liquids can exhibit superior potential windows in the range of 6V (approx. -3 to 3 V). A recent review of electrodeposition in non-aqueous systems found that elements from nearly every group have been successfully deposited in ionic liquids.[37] Notably, NuLi et al. used a nitrogen based ionic liquid, 1-butyl-3-methylimidazolium tetrafluoroborate, [BMIM]-BF_4, for the formation of the first successful deposits of magnesium at ambient temperatures.[38]

With regard to semiconductor materials, there have been several successful results reported in literature. In the early 2000's, Endres and colleagues reported several instances of nanoscale germanium deposition in the ionic liquids [BMIM]PF_6.[39,40] A few years later, this group also reported the successful deposition of nanoscale silicon in 1-butyl-1-methylpyrrolidinium bis(trifluoromethylsufonyl)amide [BMP-TFSI].[41] In the following decade, much of the work has been focused on process-oriented variables such as the identity of the cathodic electrode[34] or the use of temple-assisted deposition to create specialized structures like nanowires[42,43] or 3D ordered macroporous materials.[44]

Recently, however, it has been shown that the structure of the ionic liquids used can have a significant effect on the morphologies of deposits. Endres et al. discovered that deposition of Si_xGe_{1-x} resulted in nanoscale films in [BMP]-TFSI. In contrast, [BMIM]-TFSI produced microscale films. They proposed the possibility of different solvation layers of each ionic liquid at the electrode surface as the source of these morphological changes.[45] Furthermore, Pulletikurthi et al. showed a similar effect when differing counteranions of the same cation were employed.[46] Clearly, the structure and chemistry of each individual ionic liquid can have profound effects on the deposition.

Research Objectives

With these observations in mind, the present work was focused on the development of new phosphonium ionic liquids for the electrodeposition of silicon. As stated previously, relatively little work is evident in the literature on phosphonium ionic liquids compared to their nitrogen counterparts. This view is particularly true for electrochemistry in phosphonium ionic liquids. In 2007, Tsunashima et al. reported several new short-chain phosphonium ionic liquids with low viscosities (< 100 mPa·s) and high electrochemical stabilities.[5] The focus of that study was lithium-ion batteries, but the ionic liquids created also showed the significant cathodic stabilities needed for silicon electrodeposition. In the present work, several new phosphonium ionic liquids were synthesized and feature substituents that possess a wide variety of structural and electronic properties as illustrated in Figure 1.4. Moreover, the physical and electrochemical characteristics of each new ionic liquid were compared with those reported previously for triethyl(2-methoxyethyl)phosphonium bis(trifluoromethylsulfonyl)imide (P_{201}-TFSI).[5] Additionally, the successful

electrodeposition of nanoscale silicon in P_{201}-TFSI is also reported, along with several efforts to deposit silicon in the newly synthesized phosphonium ionic liquids.

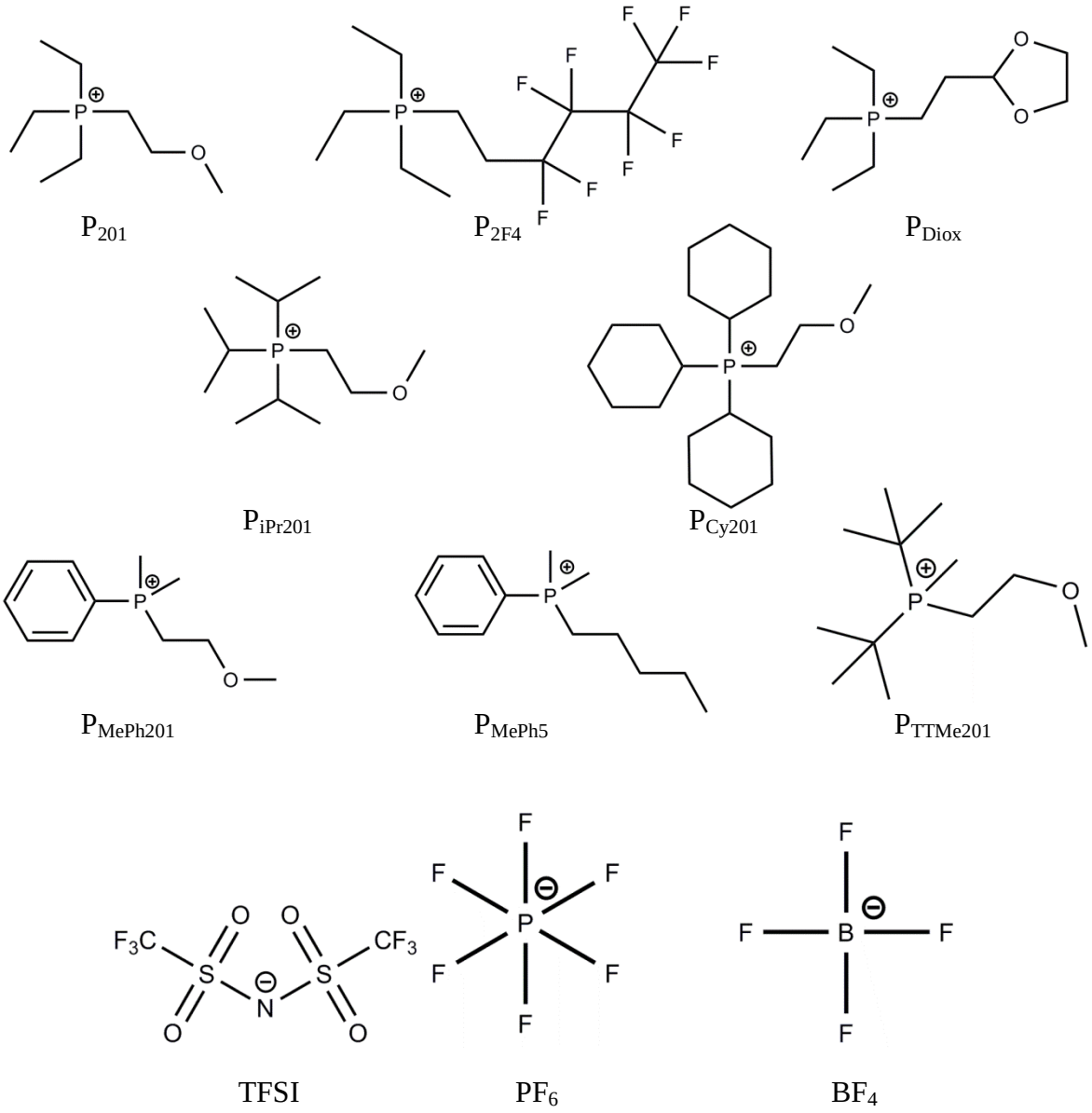

Figure 1.4: Structures of the new phosphonium cations prepared in this work, along with the three anions paired with them. Each label includes the shorthand notation that has been used throughout the rest of this work.

RESULTS AND DISCUSSION

Table 1.1: Summary of the physical properties of the new ionic liquids.

Ionic Liquid	MW[a]	$T_m/(T_g)$ °C[b]	ρ (g/ml)[c]	C (mol L^{-1})[d]	σ (mS cm^{-1})[e]	Λ (S cm^2 mol^{-1})[f]
P_{201}-TFSI[g]	458	10	1.39	3.03	3.58	1.180
-BF_4	263	9	1.34	5.10	2.85	0.559
-PF_6	322	63	1.68	5.22	0.016	0.003
P_{Diox}-TFSI	500	(-36)	1.07	2.14	0.13	0.061
-BF_4	305	(-32)	1.63	5.34	0.025	0.005
-PF_6	364	(-28)	1.19	3.27	0.020	0.006
P_{2F4}-TFSI	646	49	1.36	2.11	0.061	0.029
-BF_4	451	(53)	1.76	3.90	-	-
-PF_6	510	(66)	1.37	2.69	-	-
P_{iPr201}-TFSI	500	18	1.71	3.42	0.10	0.029
-BF_4	305	68	1.36	4.46	-	-
-PF_6	364	84	1.32	3.63	-	-
P_{Cy201}-TFSI	626	63	1.56	2.49	0.015	0.006
-BF_4	431	(92)	1.39	3.23	0.007	0.002
-PF_6	490	98	1.63	3.33	-	-
$P_{MePh201}$-TFSI	478	8	1.48	3.10	4.80	1.550
-BF_4	283	47	1.53	5.41	0.18	0.033
-PF_6	342	49	1.57	4.59	0.077	0.017
P_{MePh5}TFSI	490	< -40[h]	1.49	3.04	2.02	0.664
-BF_4	295	< -40[h]	1.34	4.54	0.36	0.079
-PF_6	354	(-16)	1.33	3.76	0.16	0.043
$P_{TTMe201}$-TFSI	506	52	1.82	3.60	0.029	0.008
-BF_4	311	(68)	1.50	4.82	0.011	0.002
-PF6	370	(75)	1.65	4.46	-	-

[a] Molecular Weight
[b] Melting point (or glass transition temperature)
[c] Density at 25 °C
[d] Concentration at 25 °C
[e] Ionic conductivity at 25 °C
[f] Molar conductivity at 25 °C
[g] Ref #5
[h] No thermal transitions detected above this temperature

The physical characteristics of ionic liquids are affected by two major factors, namely the electrostatic interactions between the cations and anions, and the crystal packing effects which, in turn, are sensitive to the steric demands of each particular phosphonium cation. A summary of the pertinent physical properties of the new ionic liquids is presented in Table 1.1.

Melting Point and Glass Transition

The melting point or glass transition temperature of an ionic liquid is one of the most important properties in terms of useful applications of ILs. In general, the use of longer alkyl chain lengths for the cationic substituents results in ionic liquids with relatively low melting points. Interestingly, the use of the short chain triethyl(2-methoxyethyl)phosphonium (P_{201}) cation has been reported to afford ionic liquids with thermal properties that are competitive with those of the widely used imidizolium and pyrollidinium based ionic liquids such as [EMIM]-TFSI and [BMP]-TFSI. The pronounced influence of the ether substituent in the case of P_{201} is attributable to the favorable crystal packing that arises as a consequence of the increased conformational freedom around the oxygen atom.[5] This effect was also reported by Zhou et al. in their study of multi-methoxy ammonium ionic liquids.[11] On this basis, the substitution of a dioxalane for the ether substituents would be anticipated to reduce the conformational freedom somewhat due to the ring structure, thereby resulting in an increase in the melting point or glass transition temperature. However, corresponding ionic liquids that feature the cation triethyl(2-ethyl-1,3-dioxolane)phosphonium (P_{Diox}) only exhibit glass transitions at low temperatures (T_g = -36 ºC for P_{Diox}-TFSI). In the case of the dioxalanes, the loss of conformational freedom may be offset by the addition of extra alkyl interactions from the dioxalanes ring itself. A few comparable studies have been reported

which utilized ring substituents. For example, Tsunashima et al. appended a benzyl substituent to triethylphosphine which afforded ionic liquids with low glass transition temperatures.[47] However, it is unclear if this property was attributable to conformational considerations that may be mirrored in the dioxalanes ring or due to electronic effects from the benzyl that would not be expected in the sp^3 dioxalane. Interestingly, the ranges of the glass transition temperatures for the three anions are smaller than would be expected on the basis of the normal trends, in which TFSI salts typically display significantly lower melting points due to the exceptional conformational freedom of the TFSI anion. This trend may indicate that the intermolecular interactions of the dioxalanes are more important than the steric and electrostatic characteristics of each anion.

The use of fluorinated substituents has proved to be useful in terms of disruption of the normal crystal packing. Moreover, the propensity of fluorinated alkyls to segregate into highly fluorinated phases has been utilized for the creation of highly hydrophobic ionic liquids with fairly low melting points.[48] For example, the triethyl(1H,1H,2H,2H-perfluorohexyl)phosphonium cation (P_{2F4}) may use a partially fluorinated substituent to induce a slight amount of fluorinated phase separation, thereby disrupting the normal crystal packing that would be expected to occur between the alkyl chains. This particular ionic liquid displays a modest melting point of 49 ºC compared to a similar alkylated analogue triethylpentylphosphonium TFSI which has a melting point at 17 ℃.[5] This observation implies that the crystal packing efficiency has probably increased as a consequence of the fluorination. While electron withdrawal from the phosphonium center also represents a plausible explanation for this result, it is noteworthy that ^{1}H NMR chemical shifts of the protons of the substituent adjacent to the phosphorus atom show essentially no pronounced deshielding (δ= 2.51 ppm) in

comparison with that of the ionic liquid triethyl(methoxymethyl)phosphonium TFSI (δ= 4.22 ppm) which has a melting point of 14 ºC. On the basis of X-ray crystallographic studies, it has been demonstrated by Tindale et al. that similar phosphonium iodide salts associate into fluorophilic and fluorophobic phases in the solid state. However, the effect of fluorine-containing anions on this separation was not investigated.[48] Due to the short length of the alkyl substituents, there may not have been any true "alkyl phase" to be disrupted, which would lead to simple segregation of the fluorinated tails into more ordered spacial groups.

Another plausible approach to modifying the crystal packing of ionic liquids is by replacement of the normal n-alkyl substituents with their branched alkyl analogues. Branched alkanes are unable to pack as efficiently as their straight chain counterparts and consequently have reduced Van der Waals forces. When this trend is applied to the alkyl substituents on a phosphonium cation, the anticipated result would be a lowering of the melting points of the following ionic liquids. In the case of tri-*i*-propyl(2-methoxyethyl)phosphonium (P_{iPr201}) TFSI, however, an increase in the melting point is observed (18 ºC). This effect has also been observed when comparing the n- and i-isomers of tributylmethylphosphonium TFSI which have melting points of 16°C and 52 °C, respectively.[6,8] If the isopropyl groups are replaced by cyclohexyl moieties (P_{Cy201}), a further increase in melting point is observed (63 ºC). Despite the increase in alkyl length and possible Van der Waals forces, the observed increases in melting point may arise from some special crystal packing in the case of P_{iPr201} that is compounded in P_{Cy201} by what can be regarded as the extension of the isopropanes into cyclohexanes. Additionally, there may be diminished conformational flexibility in the cyclohexane rings.

An underutilized strategy for enhancing the physical properties of an ionic liquid involves decreasing the symmetries of both the cation and the anion. Due to the

difficulty and expense involved in synthesizing less symmetrical phosphines of the type PR_2R', relatively little attention has been paid to phosphonium cations that are derived from them. Nevertheless, two phosphonium ionic liquids based on dimethylphenylphosphine, dimethylphenyl(2-methoxyethyl)phosphonium ($P_{MePh201}$) and dimethylphenyl(pentyl)phosphonium (P_{MePh5}) have in fact both been prepared and characterized. Despite the weaker electron donation of the phenyl group as compared with that of the alkyl counterpart, $P_{MePh201}$-TFSI exhibits a melting point of 8 ºC, which is slightly lower than that of the triethyl counterpart P_{201} -TFSI. Changing the ether substituent to a linear pentyl group resulted in a significant decrease in the melting point, such that P_{MePh5} TFSI exhibited no melting or glass transitions above -40 ºC. This observation mirrors the trends that have been observed for other phosphonium ionic liquids.[5] These results may open another avenue of study, as imidizolium salts with phenyl based substituents have been shown to exhibit a degree of electronic tunability due to the facile substituent change available to aryl systems.[49] Another less symmetric cation, di-*t*-butylmethyl(2-methoxyethyl)phosphonium ($P_{TTMe201}$) has a higher melting point (52 ºC) with the same TFSI anion compared to the previous two cations discussed above. This trend may also be attributable to the branched chain effect which is also evident in P_{iPr201} and P_{Cy201}.

The ion pairs synthesized all have transition temperatures below 100 ℃, satisfying the conventional definition of an ionic liquid. ILs with the TFSI anion were found to have the lowest transition temperatures and represented the most room-temperature ionic liquids. This observation mirrors trends seen in other ionic liquids, where the TFSI and related bis(fluorosulfonyl)amide (FSA) anions are favored in electrochemical applications. In comparison, BF_4 and PF_6 show relatively higher thermal transitions, though it should be noted that these results run countercurrent to others.

Typically, PF_6 salts have lower transitions than their BF_4 counterparts, yet every example here shows the opposite.

Conductivity

One of the most fundamental properties of any electrolyte is its conductivity. In turn, the conductivity is greatly influenced by the mobilities of the component ions which, in turn, relates to their molar volumes and viscosities. Neat ionic liquids typically display conductivities on the order of 0.1-10 mS cm^{-1} while previously reported nitrogen based Ils, such as [BMP]-TFSI and [BMIM]-TFSI exhibit relatively high conductivities of 3.78 and 5.76 mS cm^{-1}, respectively.[50] The most comparable ionic liquid previously reported is P_{201}-TFSI which has an ionic conductivity of 3.58 mS cm^{-1}. As expected, the newly synthesized room temperature ILs exhibit a strong correlation between the viscosity of the ionic liquid and the resulting conductivity. Thus, the ILs with increased viscosity display a decrease in conductivity as evident in the case of P_{Diox}-PF_6 which has a conductivity of 0.02 mS cm^{-1}. Interestingly however, $P_{MePh201}$-TFSI and P_{MePh5}-TFSI both exhibit abnormally high molar conductivites when compared to their viscosities. This may put them in a category known as "superionic" liquids, although further investigation is warranted to merit such a label.[51] All of the room temperature TFSI ILs described in the present work display conductivities in the range of 0.1-5.0 mS cm^{-1}. On the other hand, the corresponding BF_4 and PF_6 salts generally fall below that range. In the cases of ILs that exhibit melting points or glass transitions above room temperature, a correlation between the T_m/T_g and the respective conductivities is evident. As might be expected, the salts with higher melting salts generally show decreased conductivities.

Viscosity

Viscosity is also an important property when considering the use of ionic liquids as media for electrochemical studies. As expected, the diffusion of electroactive species to the electrodes is strongly influenced by the viscosity of the medium in which they are dissolved. This issue becomes especially important in the context of electrodeposition in highly viscous ionic liquids, since this obstacle can preclude their use in an industrial setting. The organic solvents that are typically used for electrochemical processes, such as acetonitrile, have very low viscosities on the order of 1 mPa·s at room temperature, while the viscosities of the least viscous ionic liquids fall within the range of approximately 20-40 mPa·s. As expected, the viscosities of the ionic liquids decrease sharply as a function of increasing temperature.

The P_{201}-TFSI ionic liquid has a low viscosity of 44 mPa·s which is attributable in part to the increased conformational flexibility of the ether substituent. Despite the low glass transition temperatures of the P_{Diox} based ionic liquids, all three salts displayed viscosities that are higher than those of trihexyl(tetradecyl)phosphonium ILs of the same type. For example, P_{Diox}-TFSI and P_{66614}-TFSI have viscosities of 737 and 450 mPa·s, respectively. The two phosphonium cations derived from dimethylphenylphosphine ($P_{MePh201}$ and P_{MePh5}) form ionic liquids with relatively moderate viscosities. For example, $P_{MePh201}$-TFSI has a viscosity of 136 mPa·s at 25 °C, a value that falls within the range reported for other highly asymmetric phosphonium ILs such as i-butyldiethylmethylphosphonium TFSI (72 mPa·s at 30°C).[8] If the ether substituent in these compounds is exchanged for a straight alkyl chain (P_{MePh5}-TFSI) the viscosity of the resulting ionic liquid increases to 331 mPa·s, thus mirroring the trend observed for other short chain phosphonium and ammonium ILs.

Electrochemical Stability

From the standpoint of electrodeposition, one of the great advantages of ILs relates to their wide electrochemical windows, which in turn allows for the deposition of a wide variety of materials. In terms of electrochemical applications, the size of this electrochemical window is the critical property. However, in the case of electrodeposition, the IL need only be stable beyond the potential needed for the desired oxidation or reduction. In the case of silicon, the four electron reduction of a Si(IV) species such as $SiCl_4$ occurs at approximately -2.4 vs. Ag QRE (quasi-reference electrode).[35] In turn, this implies that ILs for this process need to exhibit cathodic stabilities in the range of -2.4 to -3.0 V. For comparison, the nitrogen-based ILs that have been used previously for the successful deposition of elemental silicon feature cathodic stabilities of approximately -3.1V vs. Ag QRE.[41] In the present work, the cathodic and anodic limits of the newly synthesized room-temperature phosphonium ionic liquids were established on the basis of cyclic voltammetry (CV). As evident from Figure 1.5, the CVs of the purified ionic liquids are relatively featureless prior to the onset of oxidation or reduction of the ions occurred at higher potentials.

A featureless voltammogram can, in some ways, be a simple tool for qualitative analysis of the purity of ionic liquids. The most common impurity found in ionic liquids, water, displays an easily identifiable peak which corresponds to the reduction of protons to hydrogen gas. Additionally, some residual metal cations commonly used in IL synthesis such as silver will be clearly seen through the baseline background, while others such as group I cations may require potentials at the outer edge of the ionic liquid range. In previous work, it has been shown that residual halide impurities from the synthetic process can manifest in lessened electrochemical windows.[52] In the present work, ionic liquids were repeatedly extracted with water and the resulting extracts were

tested with silver nitrate. Since silver halides are very insoluble ($k_{sp} < 1x10^{-10}$), very sensitive halide detection can be achieved. The anodic, cathodic, and total electrochemical stabilities of the room-temperature phosphonium ILs that have been synthesized in the present work are summarized in Table 1.2

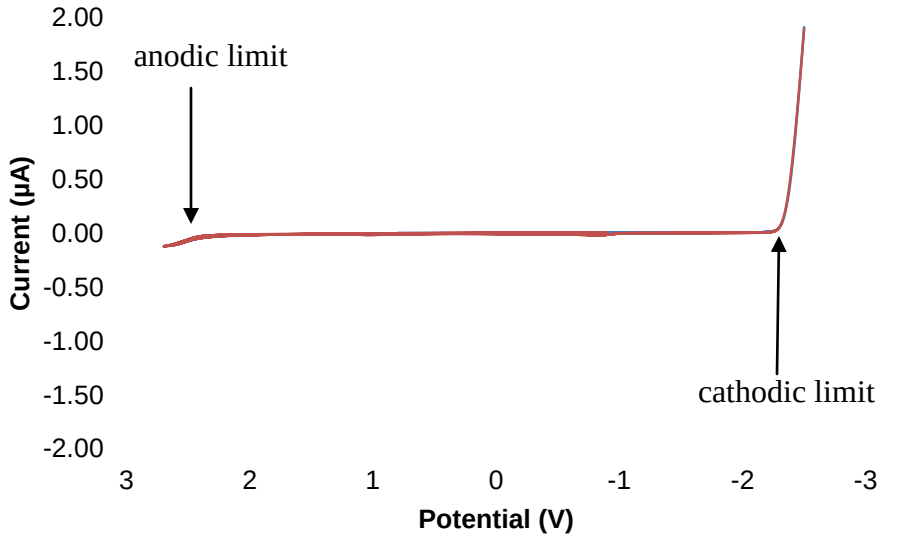

Figure 1.5: Cyclic voltammogram of P_{MePh5}-TFSI recorded at a scan rate of 50 mV/s using a 2mm Pt disk, Pt wire and Ag wire as working, counter, and quasi-reference electrodes, respectively

Table 1.2: Electrochemical stabilities of selected room-temperature phosphonium ionic liquids vs. an Ag quasi-reference electrode.

Ionic Liquid	E_{red} (V)	E_{ox} (V)	Total Window (V)
P_{201}-TFSI	-2.6	+3.0	5.6
P_{Diox}-TFSI	-1.8	+3.0	4.8
$P_{MePh201}$-TFSI	-2.1	+2.5	4.6
P_{MePh5}-TFSI	-2.4	+2.5	4.9

All the phosphonium ILs that were tested exhibited wide electrochemical windows of approximately 5 V. Typically, the presence of the ether substituent in P_{201}-TFSI decreases the viscosity of this ionic liquid. However, it has also been shown to reduce the electrochemical stability of the cation in comparison with that of triethylpentylphosphonium-TFSI which displays a cathodic limit that is approximately 300 mV higher.[5] Nevertheless, the ionic liquid P_{201}-TFSI possesses a wide window of 5.6V that is comparable with those of other nitrogen-based ILs. Moreover, the reduction of this ionic liquid takes place at a higher potential that that of silicon. By contrast, P_{Diox}-TFSI is a very viscous liquid with a low glass transition temperature which generally correlates with increased electrochemical stability. Interestingly, while this IL has a total window of 4.8V, the cathodic limit is reduced to -1.8 V vs. Ag QRE. It is unclear at this point whether this process involves the reduction of the phosphonium cation or a reduction of the dioxolane substituent in some fashion. The ILs based on dimethylphenylphosphine, $P_{MePh201}$-TFSI and P_{MePh5}-TFSI, possess wide windows of 4.6 and 4.9V, respectively. P_{MePh5}-TFSI exhibits a cathodic limit at -2.4 V vs. Ag QRE that lies at the limit of the desired range for silicon deposition. On the other hand, $P_{MePh201}$-TFSI displays a reduced total window and stability with respect to reduction in comparison with that of the pentyl analogue, thus mirroring the trend noted earlier for P_{201}-TFSI. Comparison of the TFSI salts of P_{201} and $P_{MePh201}$ reveals the electrochemical effect of the presence of alkyl substituents on the phosphonium center versus those of the less electron donating phenyl group. The conspicuous difference between the two ionic liquids implies that phosphonium ILs featuring more than one phenyl substituent may be less suitable for electrochemical processes at highly reductive potentials.

Electrodeposition of Silicon

Figures 1.6-1.8 shows the cyclic voltammogram of a 2 mm diameter platinum disk electrode immersed in the ionic liquid P_{201}-TFSI along with three different silicon chloride compounds. The addition of each silicon chloride compounds resulted in the appearance of a distinct reduction peak at approximately -2 V (vs. Ag QRE). Prior to this, a weak, broad peak was observed at the beginning of negative potential scan. This peak corresponds to the reduction of protons which are produced by the reaction of the silicon chloride compounds with the trace amount of residual water in the ionic liquid as expressed in following equation.[35]

$$SiX_4 + 2H_2O \rightarrow SiO_2 + 4HX$$

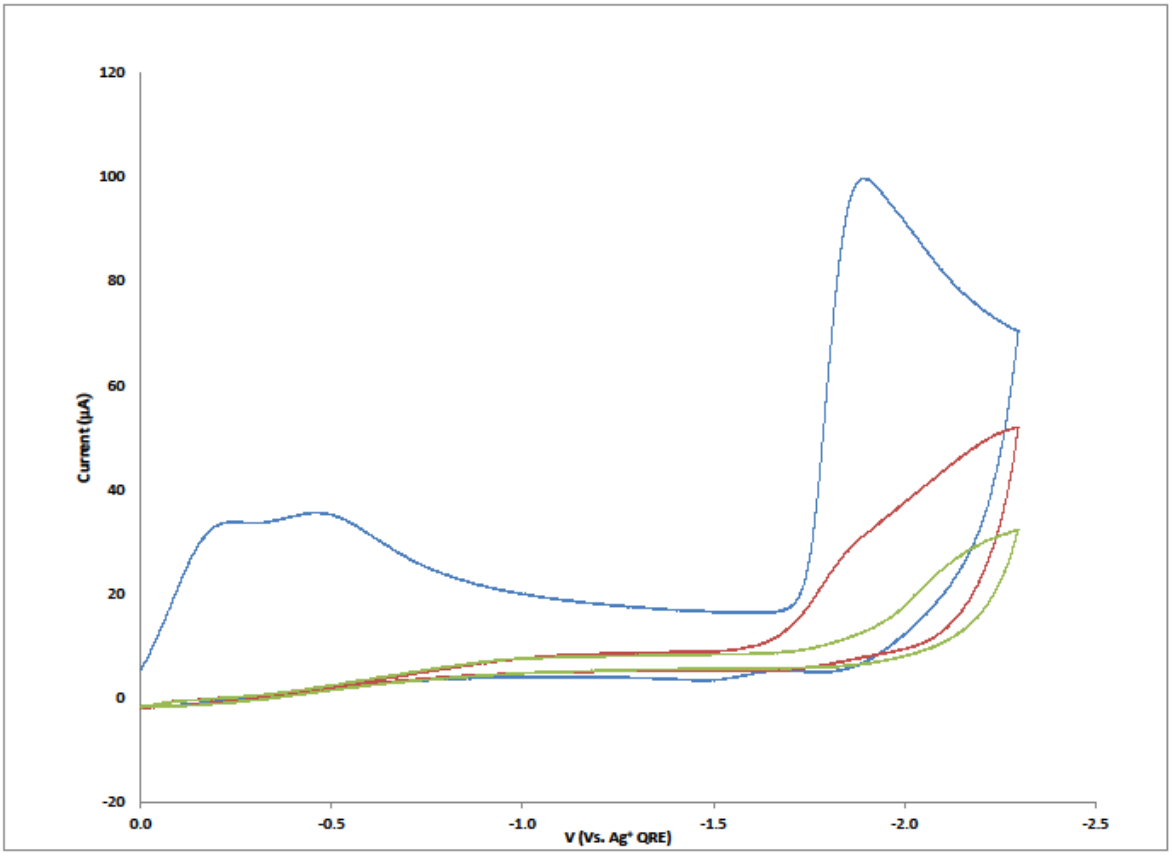

Figure 1.6: Cyclic voltammograms of $SiCl_4$ in the ionic liquid P_{201}-TFSI using a Pt disk electrode of 2mm diameter and a scan rate of 100 mV/s.

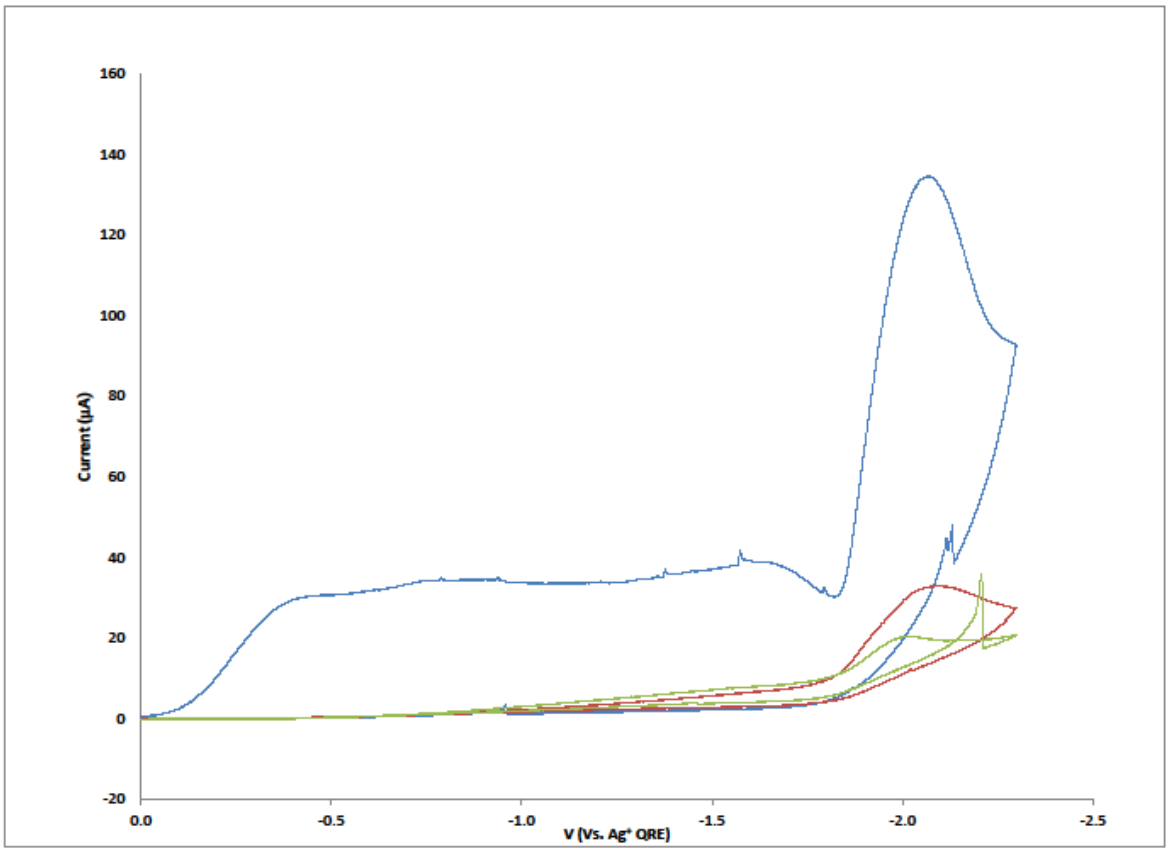

Figure 1.7: Cyclic voltammograms of $SiHCl_3$ in the ionic liquid P_{201}-TFSI using a Pt disk electrode of 2 mm diameter and a scan rate of 100 mV/s.

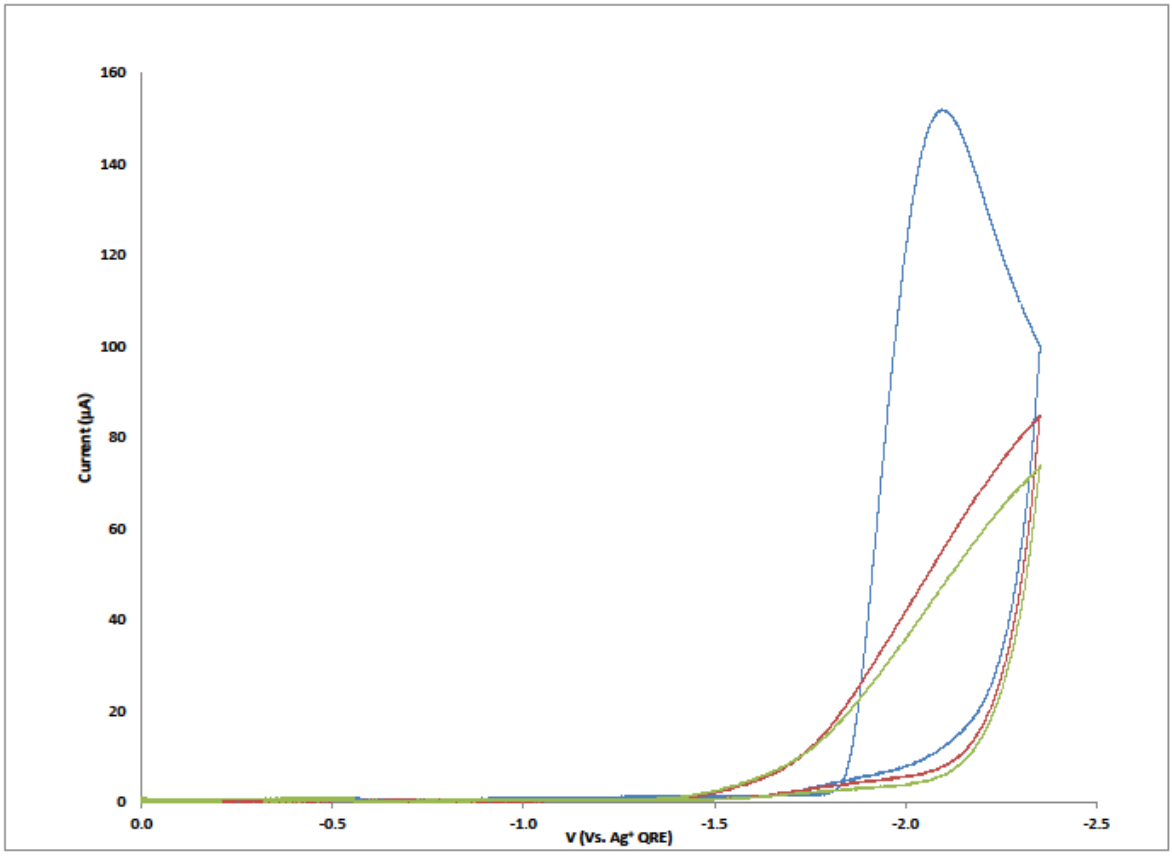

Figure 1.8: Cyclic voltammograms of Si_2Cl_6 in the ionic liquid P_{201}-TFSI using a Pt disk electrode of 2 mm diameter and a scan rate of 100 mV/s.

Interestingly, Si_2Cl_6 did not exhibit a proton reduction peak since, unlike the other silicon precursors, it is not reactive with water. In contrast to the intense reduction peaks, the corresponding oxidation peaks did not appear in the reverse scan, thus implying that the reduced silicon species do not dissolve electrochemically in the ionic liquid. Attenuation of the reduction peaks was observed after each consecutive scan. This

observation is very similar that observed for the electrodeposition of silicon from organic solvents.[35,53] The two systems differ, however, in regard to the peak current. An equal level of current at the reduction peak was observed in the case of only 10 mM silicon tetrachloride in acetonitrile solution on the same electrode area. This is due to the difference in the diffusion coefficients in association with the viscosities of the two solutions. Unfortunately, it is not simple to derive the diffusion coefficients of the silicon chloride compounds from the peak currents because of the complexity of the corresponding four-electron reduction reaction. Such reactions involve a multiple electron transfer process which is in conjugation with a chemical reaction; namely, the removal of the chloride ion. Furthermore, the electrode surface becomes gradually passivated due to the presence of the silicon deposit. (Fig. 1.9).[29] From the equation,

$$i_{ss} = 4nFC_O^* D_O r$$

where n is the number of electron involved, and F is Faraday constant, and C_O^* is the concentration of the reactant, and D_O is the diffusion coefficient of the reactant, and r is the radius of UME disk, the diffusion coefficient of $SiCl_4$ was estimated to 1.3×10^{-8} cm^2/s. This value is more acceptable than the values in the range of $10^{-10} \sim 10^{-11}$ cm^2/s that were obtained from the general CV peak condition on the 2 mm platinum disk. It is speculated that the current becomes smaller with a UME with the result that passivation by the deposit was less severe.

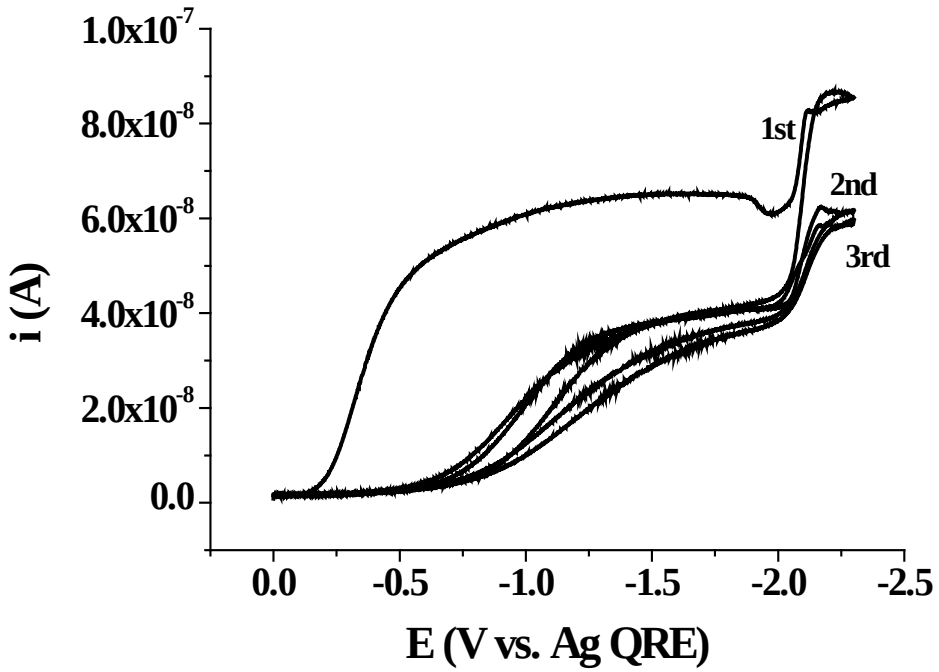

Figure 1.9: Cyclic voltammogram of P_{201}-TFSI containing 1.0 M $SiCl_4$ on a 25 μm Pt ultramicroelectrode (UME) with a scan rate of 20 mV/s.

Figures 1.10-1.12 display SEM images of the surfaces of the materials deposited from each silicon chloride compound in P_{201}-TFSI. EDS analyses (see Table 1.3) confirmed that in each case a silicon layer had been formed with a low level of impurity (below the detection limit). The deposited films were smooth and continuous in contrast to the silicon deposits that have been made from other ionic liquids which feature granular surfaces.[41,54,55] As observed in the case of other organic solvents, the silicon deposits were readily oxidized on exposure to air. Interestingly, the deposit from $SiHCl_3$, which features a hydrogen-silicon bond (Si-H) was found to be resistant to oxidation for a few hours. Examination of products by XRD revealed that the deposits are amorphous, and are similar to silicon that has been electrodeposited from other organic solvents or ionic liquids.[34,35,41,53–55]

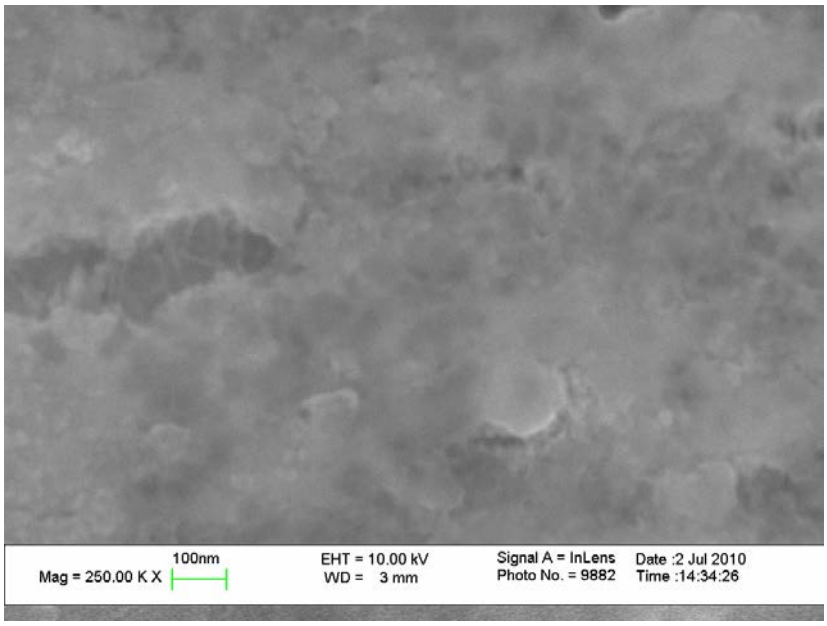

Figure 1.10: SEM images of silicon electrodeposited from P_{201}-TFSI containing 1.0 M $SiCl_4$ on a silver substrate with an applied potential of -2.2 V (vs. Ag QRE) for 1000 s.

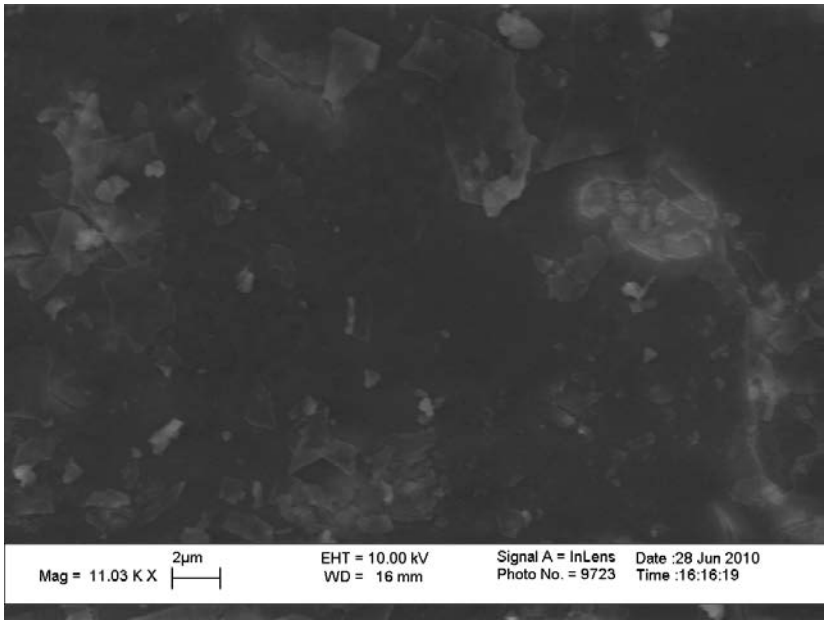

Figure 1.11: SEM images of silicon electrodeposited from P_{201}-TFSI containing 1.0 M $SiHCl_3$ on a molybdenum substrate with an applied potential of -2.1 V (vs. Ag QRE) for 1000 s.

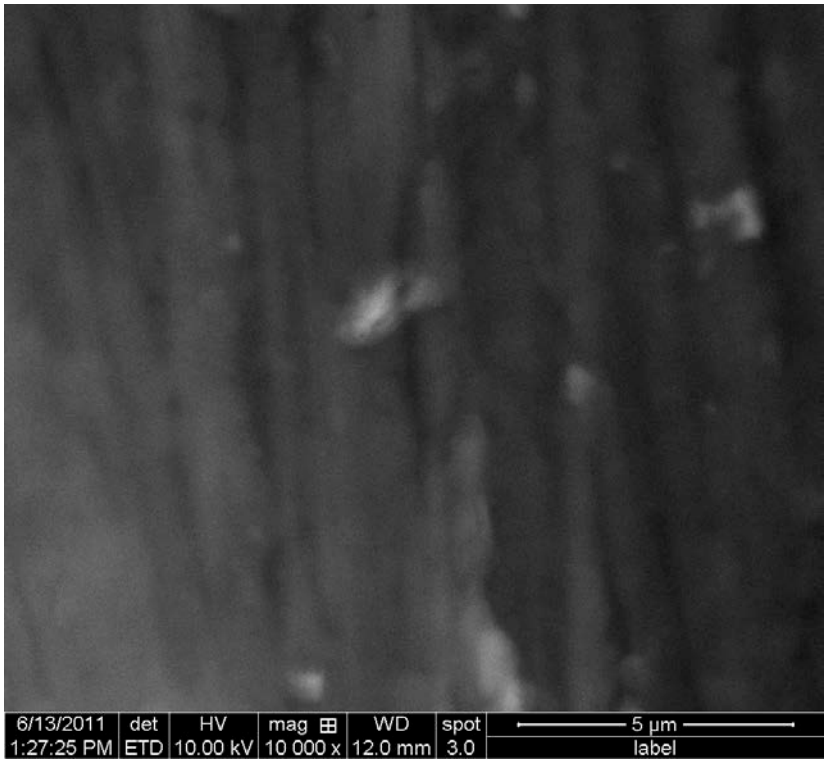

Figure 1.12: SEM images of silicon electrodeposited from P_{201}-TFSI containing 1.0 M Si_2Cl_6 on a nickel substrate with an applied potential of -2.1 V (vs. Ag QRE) for 500 s.

Table 1.3. Elemental compositions of the silicon electrodeposits as obtained by EDS.

Element (in at.%)	$SiCl_4$	$SiHCl_3$	Si_2Cl_6
Si	10.8	29.2	20.2
Cl	0.0	0.0	0.0
C	9.4	0.0	4.2
O	23.7	0.0	56.3
P	1.2	0.0	0.0
F	0.0	0.0	0.0
Substrate	54.8	70.8	19.2

High purity in the resultant film would be of utmost importance in true industrial application of electrodeposition. It can be seen that all three deposits exhibit a low level of contamination from the ionic liquid itself, with carbon, phosphorus, and fluorine levels below 10 atomic %. This level of contamination relates directly to the cathodic stability of the solvent used; as the potential is increased it is more likely for products of electrochemical degradation to be present and contribute to the level of impurities. This issue can be of major concern in organic solvents, where carbon contamination from something such as CH_2Cl_2 can be as high as 28 at. %.[36] Nevertheless, the most troubling aspect of silicon electrodeposition to date is the presence of oxygen impurities. In the cases of the $SiCl_4$ and Si_2Cl_6 films, oxygen is present at an almost 2:1 ratio with regards to silicon. This outcome may be due to the two key properties of the films themselves, thickness and morphology. Oxygen can only bind to silicon on open sites near the surface of the film, hence, thinner films tend to show a larger oxygen/silicon ratio due to having a larger surface area/volume ratio. Additionally, any penetration by oxygen into the film has a greater effect at smaller thickness. Morphologically, amorphous materials tend to have more open binding sites than crystalline or semi-crystalline materials, thus leading to higher oxygen contents. As such, high temperature annealing may further enhance the purity of films. It should be noted, however, that the films produced in the present work were made in an inert atmosphere glove box and the only exposure to oxygen occurs during transfer of the film to appropriate instruments for analysis. As a consequence, processes such as annealing should be carried out in the original inert atmosphere whenever possible. An interesting alternative to this approach is built in chemical resistance such as that found on the $SiHCl_3$ film. This resistance may be due to residual hydrogen atoms occupying the open silicon binding sites on the film's

surface.[34,35,53,54] The small size of the hydrogen atom makes it difficult to detect in surface elemental analysis techniques such as EDS.

CONCLUSIONS

Over twenty new short-chain phosphonium ionic liquids with a variety of electronic and structural properties have been synthesized and used for the electrodeposition of silicon including several new room-temperature ionic liquids. The physical and electrochemical properties of the ILs were found to have a strong dependence on the nature of substituents on the phosphonium cation. Generally speaking, the phosphonium ionic liquids were found to follow the same design trends found in their nitrogen-based counterparts. Phosphonium cations with branched alkyl chains or cyclic substituents were shown to have less desirable thermal properties than those of their n-alkyl analogues. Futhermore, a new class of less symmetrical cation based on dimethylphenylphosphine showed promising characteristics and is a candidate for future studies. Electrochemically, a few of the newly synthesized phosphonium ionic liquids displayed the potential window necessary for silicon deposition. Nanoscale thin films of silicon were successfully deposited by electrochemical reduction of the silicon precursors $SiCl_4$, $SiHCl_3$ and Si_2Cl_6 in the known ionic liquid P_{201}-TFSI. In each case, the deposited silicon featured a smooth morphology and an amorphous structure in contrast to the cracked and granular films that have been deposited using other nitrogen-based ionic liquids. Interestingly, it was also discovered that the silicon films deposited from $SiHCl_3$ exhibited more resistance to oxidation than those deposited from aprotic silicon precursors, possibly due to the H-termination of open silicon binding sites present on the film surface.

EXPERIMENTAL

General Considerations

Triethylphosphine, di-t-butylmethylphosphine, triisopropylphosphine, triclyclohexylphosphine and dimethylphenylphosphine were purchased from Strem Chemicals, Inc. while LiTFSI, $NaBF_4$, $NaPF_6$, alkyl halides and silicon precursors were all purchased from Sigma-Aldrich Inc. All chemicals were of the highest available purity and used as received. All phosphonium syntheses were performed under a dry, oxygen-free argon atmosphere or vacuum using standard Schlenk line and dry box techniques. All glassware was dried at least 24 h in a 120 °C oven prior to use. Toluene was distilled over sodium with a sodium benzophenone ketyl indicator and was degassed before use. Dichloromethane was distilled over calcium hydride.

Instrumentation

The NMR spectra were recorded on a Varian 300 Unity Plus spectrometer (300 MHz, 298K). For ^{1}H and ^{13}C spectra, chemical shifts are referenced to the deuterated solvent while CHF_3 and H_3PO_4 were used for ^{19}F and ^{31}P, respectively. Melting points and glass transition temperatures were found using a TA Instruments Q100 Differential Scanning Calorimeter in a range of -40 to 150 ℃ at a scan rate of 5 ℃/min. Viscosity was measured using an A&D Company SV-10 Vibroviscometer at 25 ℃. Conductivity was calculated by impedance spectroscopy using an Eco Chemie. B.V. PGSTAT302N Autolab. Density was calculated by gravimetric analysis using a calibrated pipette. The silicon deposits were examined with a FEI Company Quanta 650 FEG scanning electron microscope, and the composition of each Si deposit was established on the basis of a Bruker XFlash® Detector 5010 utilizing energy dispersive spectroscopy.

Electrochemistry

All electrochemistry experiments were performed in an Ar gas-filled glove box (Vacuum Atmospheres Corp., Hawthorne, CA). The cyclic voltammetry studies (CV) and silicon electrodepositions were carried out with a CH Instruments Model 660 Electrochemical Workstation. The working electrode was a 2 mm platinum disk or a 25 μm diameter platinum ultramicroelectrode (UME). The UME was polished with three different grades of alumina (1, 0.3, and 0.05 μm), sonicated in deionized water and rinsed with acetone prior to conducting the experiments. Molybdenum foil (0.025 cm thick, 99.94%, Alfa Aesar, Ward Hill, MA) and silver foil (0.0127 cm thick, 99.9%, Alfa Aesar, Ward Hill, MA) were also used as working electrodes. The counter electrode was a platinum wire (0.1 cm diameter, Alfa Aesar, Ward Hill, MA) and the reference electrode was a silver wire (0.1 cm diameter, Alfa Aesar, Ward Hill, MA) which was used as a quasi reference electrode (QRE). The potential of the QRE was a reasonably stable and the measured potential varied within ±5 mV.

Synthesis of Phosphonium Halides

Triethyl(2-methoxyethyl)phosphonium bromide (P_{201}-Br)

Under an inert argon atmosphere, 2.94 g of (2-bromoethyl)methyl ether and 2.50 g of triethylphosphine were combined in a solution of dry, distilled toluene (50 mL). The stirred reaction mixture was allowed to reflux under an inert atmosphere overnight. The resulting P_{201}-Br colorless precipitate was then filtered, washed several times with hexanes, and dried under vacuum. Yield: 4.02 g (74%) ^{1}H ($CDCl_3$, ppm) δ: 1.12 (m, 9H, $CH_2\mathit{CH_3}$), 2.31 (m, 6H, $\mathit{CH_2}CH_3$), 2.69 (m, 2H, $\mathit{CH_2}CH_2$), 3.17 (s, 3H,

CH_3O), 3.61 (m, 2H, OCH_2) $^{13}C\{^1H\}$ ($CDCl_3$, ppm) δ: 5.49 ($CH_2\mathit{CH_3}$), 12.65 ($\mathit{CH_2}CH_3$), 19.14 ($\mathit{CH_2}CH_2$), 59.07 (CH_3O), 65.10 (OCH_2) ^{31}P ($CDCl_3$, ppm) δ: 40.13

Triethyl(1H,1H,2H,2H-perfluorohexyl)phosphonium iodide (P_{2F4}-I)

Under an inert argon atmosphere, 5.04 g of 1H,1H,2H,2H-perfluorohexyliodide and 1.56 g of triethylphosphine were combined in a solution of dry, distilled toluene (50 mL). The stirred reaction mixture was allowed to reflux under an inert atmosphere overnight. The resulting P_{2F4}-I orange precipitate was then filtered, washed several times with hexanes, and dried under vacuum. Yield: 5.28 g (80%) ^1H ($CDCl_3$, ppm) δ: 1.32 (m, 9H, $CH_2\mathit{CH_3}$), 2.53-2.87 (b, 10H, CH_2), $^{13}C\{^1H\}$ ($CDCl_3$, ppm) δ: 5.82 ($CH_2\mathit{CH_3}$), 12.55 ($\mathit{CH_2}CH_3$), 19.34 ($P\mathit{CH_2}CH_2$), 24.14 ($PCH_2\mathit{CH_2}$) ^{31}P ($CDCl_3$, ppm) δ: 40.97 $^{19}F\{^1H\}$ δ: -81.50 (3F), -115.02 (2F), -123.86 (2F), -126.43 (2F)

Triethyl(2-ethyl-3,5-dioxolane)phosphonium bromide(P_{Diox}-Br)

Under an inert argon atmosphere, 3.05 g of 2-(2-bromoethyl)-1,3-dioxolane and 1.97 g of triethylphosphine were combined in a solution of dry, distilled toluene (50 mL). The stirred reaction mixture was allowed to reflux under an inert atmosphere overnight. The resulting P_{Diox}-Br brown precipitate was then filtered, washed several times with hexanes, and dried under vacuum. Yield: 4.36 g (87%) ^1H ($CDCl_3$, ppm) δ: 1.12 (m, 9H, $CH_2\mathit{CH_3}$), 1.86 (m, 2H, $CH\mathit{CH_2}$), 2.35 (m, 8H, $P\mathit{CH_2}$), 3.79 (m, 4H, CH_2O), 4.83 (m, 1H, $O\mathit{CH}CH_2$) $^{13}C\{^1H\}$ ($CDCl_3$, ppm) δ: 5.49 ($CH_2\mathit{CH_3}$), 12.25 ($\mathit{CH_2}CH_3$), 24.94 ($OCH\mathit{CH_2}$), 64.71 (CH_2O), 101.36 ($O\mathit{CH}CH_2$) ^{31}P ($CDCl_3$, ppm) δ: 40.66

Di-tert-butylmethyl(2-methoxyethyl)phosphonium bromide ($P_{TTMe201}$-Br)

Under an inert argon atmosphere, 3.48 g of (2-bromoethyl)methyl ether and 4.01 g of di-tert-butylmethylphosphine were combined in a solution of dry, distilled toluene (50 mL). The stirred reaction mixture was allowed to reflux under an inert atmosphere overnight. The resulting $P_{TTMe201}$-Br colorless precipitate was then filtered, washed several times with hexanes, and dried under vacuum. Yield: 3.52 g (47%) ^{1}H ($CDCl_3$, ppm) δ: 1.30 (d, 18H, CCH_3), 1.85 (d, 3H, PCH_3), 2.63 (m, 2H, CH_2CH_2), 3.17 (s, 3H, CH_3O), 3.68 (m, 2H, OCH_2) $^{13}C\{^{1}H\}$ ($CDCl_3$, ppm) δ: 13.52 (PCH_3), 33.09 (CCH_3), 18.01 (CH_2CH_2), 58.19 (CH_3O), 65.68 (OCH_2) ^{31}P ($CDCl_3$, ppm) δ: 48.63

Dimethylphenyl(2-methoxyethyl)phosphonium bromide ($P_{MePh201}$-Br)

Under an inert argon atmosphere, 3.10 g of (2-bromoethyl)methyl ether and 1.56 g of dimethylphenylphosphine were combined in a solution of dry, distilled toluene (50 mL). The stirred reaction mixture was allowed to reflux under an inert atmosphere overnight. The resulting $P_{MePh201}$-Br colorless precipitate was then filtered, washed several times with hexanes, and dried under vacuum. Yield: 4.65 g (78%) ^{1}H ($CDCl_3$, ppm) δ: 2.45 (d, 6H, PCH_3), 3.26 (m, 2H, CH_2CH_2), 3.15 (s, 3H, CH_3O), 3.55 (m, 2H, OCH_2), 7.55 (m, 3H, Ar-H), 7.97 (m, 2H, Ar-H) $^{13}C\{^{1}H\}$ ($CDCl_3$, ppm) δ: 10.02 (PCH_3), 25.71 (CH_2CH_2), 59.02 (CH_3O), 65.97 (OCH_2), 120.99, 129.97, 131.82, 134. 38 (Ar) ^{31}P ($CDCl_3$, ppm) δ: 25.73

Dimethylphenylpentylphosphonium bromide (P_{MePh5}-Br)

Under an inert argon atmosphere, 3.45 g of 1-bromopentane and 2.98 g of dimethylphenylphosphine were combined in a solution of dry, distilled toluene (50 mL).

The stirred reaction mixture was allowed to reflux under an inert atmosphere overnight. The resulting P_{MePh5}-Br colorless precipitate was then filtered, washed several times with hexanes, and dried under vacuum. Yield: 5.34 g (83%) ^{1}H ($CDCl_3$, ppm) δ: 0.71 (d, 3H, CH_3CH_2), 1.10-1.43 (m, 6H, pentyl CH_2), 2.45 (d, 6H, PCH_3), 2.87 (m, 2H, PCH_2CH_2), 7.55 (m, 3H, Ar-H), 7.97 (m, 2H, Ar-H) $^{13}C\{^{1}H\}$ ($CDCl_3$, ppm) δ: 5.61 (pentyl CH_3), 8.12 (PCH_3), 13.17 (CH_3CH_2), 17.15 ($CH_2CH_2CH_2$) 21.25 (PCH_2CH_2), 23.19 (PCH_2CH_2), 120.99, 129.97, 131.82, 134. 38 (Ar) ^{31}P ($CDCl_3$, ppm) δ: 26.12

Tri-iso-butyl(2-methoxyethyl)phosphonium bromide (P_{iPr201}-Br)

Under an inert argon atmosphere, 2.63 g of (2-bromoethyl)methyl ether and 3.05 g of tri-iso-propylphosphine were combined in a solution of dry, distilled toluene (50 mL). The stirred reaction mixture was allowed to reflux under an inert atmosphere overnight. The resulting P_{iPr201}-Br colorless precipitate was then filtered, washed several times with hexanes, and dried under vacuum. Yield: 4.77 g (85%) ^{1}H ($CDCl_3$, ppm) δ: 1.10 (m, 18H, $CHCH_3$), 2.50-2.69 (m, 5H, $CHCH_3$, PCH_2), 3.05 (s, 3H, CH_3O), 3.47 (m, 2H, OCH_2) $^{13}C\{^{1}H\}$ ($CDCl_3$, ppm) δ: 16.40 ($CHCH_3$), 20.47 ($CHCH_3$), 21.03 (CH_2CH_2), 58.34 (CH_3O), 65.10 (OCH_2) ^{31}P ($CDCl_3$, ppm) δ: 44.95

Tricyclohexyl(2-methoxyethyl)phosphonium bromide (P_{Cy201}-Br)

Under an inert argon atmosphere, 2.49 g of (2-bromoethyl)methyl ether and 4.97 g of dimethylphenylphosphine were combined in a solution of dry, distilled toluene (50 mL). The stirred reaction mixture was allowed to reflux under an inert atmosphere overnight. The resulting P_{Cy201}-Br colorless precipitate was then filtered, washed several times with hexanes, and dried under vacuum. Yield: 5.34 g (71%) ^{1}H

($CDCl_3$, ppm) δ: 1.10-1.95 (m, 33H, Cy), 2.50-2.73 (m, 5H, *CH*Cy, PCH_2), 3.28 (s, 3H, CH_3O), 3.69 (m, 2H, OCH_2) $^{13}C\{^1H\}$ ($CDCl_3$, ppm) δ: 25.71 (PCH_2*CH_2*), 26.65 (P*CH_2*CH_2), 29.93 (P*CH*Cy), 39.7-41.1 (Cy), 58.79 (CH_3O), 65.54 (OCH_2) ^{31}P ($CDCl_3$, ppm) δ: 26.12

Synthesis of TFSI ionic liquids

Triethyl(2-methoxyethyl)phosphonium bis(trifluoromethylsulfonyl)imide (P_{201}-TFSI)

4.5 g of P_{201}-Br and 5.0 g of LiTFSI were combined in water and stirred for several hours. Dichloromethane (10 mL) was added and the aqueous layer was removed. The organic layer was washed repeatedly with deionized water until the extract showed no visible precipitation with $AgNO_3$. The DCM was then removed under vacuum and the ionic liquid was dried at vacuum at 100℃ until no residual water was seen by NMR or CV. Yield: 7.95 g (98%) ^1H ($CDCl_3$, ppm) δ: 1.23 (m, 9H, CH_2*CH_3*), 2.21 (m, 6H, *CH_2*CH_3), 2.69 (m, 2H, *CH_2*CH_2), 3.29 (s, 3H, CH_3O), 3.65 (m, 2H, OCH_2) $^{13}C\{^1H\}$ ($CDCl_3$, ppm) δ: 5.49 (CH_2*CH_3*), 12.65 (*CH_2*CH_3), 19.14 (*CH_2*CH_2), 59.07 (CH_3O), 65.10 (OCH_2) 119 (m, TFSI) ^{31}P ($CDCl_3$, ppm) δ: 40.13 $^{19}F\{^1H\}$ ($CDCl_3$, ppm) δ: -79.9

Triethyl(1H,1H,2H,2H-perfluorohexyl)phosphonium bis(trifluoromethylsulfonyl)imide (P_{2F4}-TFSI)

2.5 g of P_{2F4}-I and 1.61 g of LiTFSI were combined in water and stirred for several hours. Dichloromethane (10 mL) was added and the aqueous layer was removed. The organic layer was washed repeatedly with deionized water until the extract showed no visible precipitation with $AgNO_3$. The DCM was then removed under vacuum and the ionic liquid was dried at vacuum at 100℃ overnight. Yield: 3.55 g (97%) ^1H

($CDCl_3$, ppm) δ: 1.32 (m, 9H, CH_2CH_3), 2.30-2.53 (b, 10H, CH_2), $^{13}C\{^1H\}$ ($CDCl_3$, ppm) δ: 5.82 (CH_2CH_3), 12.55 (d, CH_2CH_3), 19.34 (d, PCH_2CH_2), 24.14 (s, PCH_2CH_2) 119 (m, TFSI) ^{31}P ($CDCl_3$, ppm) δ: 40.97 $^{19}F\{^1H\}$ δ: -79.9 (TFSI), -81.50 (3F), -115.02 (2F), -123.86 (2F), -126.43 (2F)

Triethyl(2-ethyl-3,5-dioxolane)phosphonium bis(trifluoromethylsulfonyl)imide (P_{Diox}-TFSI)

2.5 g of P_{Diox}-Br and 2.5 g of LiTFSI were combined in water and stirred for several hours. Dichloromethane (10 mL) was added and the aqueous layer was removed. The organic layer was washed repeatedly with deionized water until the extract showed no visible precipitation with $AgNO_3$. The DCM was then removed under vacuum and the ionic liquid was dried at vacuum at 100℃ overnight. Yield: 4.20 g (96%) ^1H ($CDCl_3$, ppm) δ: 1.22 (m, 9H, CH_2CH_3), 1.92 (m, 2H, $CHCH_2$), 2.19 (m, 8H, PCH_2), 3.83 (m, 4H, CH_2O), 4.93 (m, 1H, $OCHCH_2$) $^{13}C\{^1H\}$ ($CDCl_3$, ppm) δ: 5.49 (CH_2CH_3), 12.25 (d, CH_2CH_3), 24.94 (s, $OCHCH_2$), 64.71 (s, CH_2O), 101.36 (d, $OCHCH_2$) 119 (m, TFSI) ^{31}P ($CDCl_3$, ppm) δ: 40.66 $^{19}F\{^1H\}$ ($CDCl_3$, ppm) δ: -79.9

Di-tert-butylmethyl(2-methoxyethyl)phosphonium bis(trifluoromethylsulfonyl)imide ($P_{TTMe201}$-TFSI)

1.81 g of $P_{TTMe201}$-Br and 1.73 g of LiTFSI were combined in water and stirred for several hours. Dichloromethane (10 mL) was added and the aqueous layer was removed. The organic layer was washed repeatedly with deionized water until the extract showed no visible precipitation with $AgNO_3$. The DCM was then removed under vacuum and the ionic liquid was dried at vacuum at 100℃ overnight. Yield: 2.95 g (97%) ^1H ($CDCl_3$, ppm) δ: 1.45 (d, 18H, CCH_3), 1.85 (d, 3H, PCH_3), 2.45 (m, 2H, CH_2CH_2), 3.35

(s, 3H, CH_3O), 3.75 (m, 2H, OCH_2) $^{13}C\{^1H\}$ ($CDCl_3$, ppm) δ: 13.52 (PCH_3), 33.09 (d, C*CH_3*), 18.01 (d, *CH_2*CH_2), 58.19 (s, CH_3O), 65.68 (m, OCH_2) 119 (m, TFSI) ^{31}P ($CDCl_3$, ppm) δ: 48.63 $^{19}F\{^1H\}$ ($CDCl_3$, ppm) δ: -79.9

Dimethylphenyl(2-methoxyethyl)phosphonium bis(trifluoromethylsulfonyl)imide ($P_{MePh201}$-TFSI)

2.5 g of $P_{MePh201}$-Br and 2.83 g of LiTFSI were combined in water and stirred for several hours. Dichloromethane (10 mL) was added and the aqueous layer was removed. The organic layer was washed repeatedly with deionized water until the extract showed no visible precipitation with $AgNO_3$. The DCM was then removed under vacuum and the ionic liquid was dried at vacuum at 100℃ overnight. Yield: 4.61 g (97%) ^1H ($CDCl_3$, ppm) δ: 2.18 (d, 6H, PCH_3), 2.76 (m, 2H, CH_2CH_2), 3.21 (s, 3H, CH_3O), 3.65 (m, 2H, OCH_2), 7.55 (m, 3H, Ar-H), 7.97 (m, 2H, Ar-H) $^{13}C\{^1H\}$ ($CDCl_3$, ppm) δ: 10.02 (PCH_3), 25.71 (d, CH_2CH_2), 59.02 (s, CH_3O), 65.97 (m, OCH_2), 119 (m, TFSI), 120.99, 129.97, 131.82, 134. 38 (Ar) ^{31}P ($CDCl_3$, ppm) δ: 25.73$^{19}F\{^1H\}$ ($CDCl_3$, ppm) δ: -79.9

Dimethylphenylpentylphosphonium bis(trifluoromethylsulfonyl)imide (P_{MePh5}-TFSI)

2.5 g of P_{MePh5}-Br and 2.78 g of LiTFSI were combined in water and stirred for several hours. Dichloromethane (10 mL) was added and the aqueous layer was removed. The organic layer was washed repeatedly with deionized water until the extract showed no visible precipitation with $AgNO_3$. The DCM was then removed under vacuum and the ionic liquid was dried at vacuum at 100℃ overnight. Yield: 4.67 g (98%) ^1H ($CDCl_3$, ppm) δ: 0.71 (d, 3H, *CH_3*CH_2), 1.10-1.43 (m, 6H, pentyl CH_2), 2.45 (d, 6H,

PCH_3), 2.87 (m, 2H, P*CH*$_2$$CH_2$), 7.55 (m, 3H, Ar-H), 7.97 (m, 2H, Ar-H) $^{13}C\{^1H\}$ ($CDCl_3$, ppm) δ: 5.61 (pentyl CH_3), 8.12 (PCH_3), 13.17 (s, CH_3*CH*$_2$), 17.15 (CH_2*CH*$_2$$CH_2$) 21.25 (d, PCH_2*CH*$_2$), 23.19 (d, P*CH*$_2$$CH_2$), 119 (m, TFSI), 120.99, 129.97, 131.82, 134. 38 (Ar) ^{31}P ($CDCl_3$, ppm) δ: 26.12 $^{19}F\{^1H\}$ ($CDCl_3$, ppm) δ: -79.9

Tri-iso-butyl(2-methoxyethyl)phosphonium bis(trifluoromethylsulfonyl)imide (P_{iPr201}-TFSI)

1.5 g of P_{iPr201}-Br and 1.5 g of LiTFSI were combined in water and stirred for several hours. Dichloromethane (10 mL) was added and the aqueous layer was removed. The organic layer was washed repeatedly with deionized water until the extract showed no visible precipitation with $AgNO_3$. The DCM was then removed under vacuum and the ionic liquid was dried at vacuum at 100°C overnight. Yield: 2.50 g (94%) ^1H ($CDCl_3$, ppm) δ: 1.10 (m, 18H, CH*CH*$_3$), 2.50-2.69 (m, 5H, *CH*CH_3, PCH_2), 3.05 (s, 3H, CH_3O), 3.47 (m, 2H, OCH_2) $^{13}C\{^1H\}$ ($CDCl_3$, ppm) δ: 16.40 (CH*CH*$_3$), 20.47 (d, *CH*CH_3), 21.03 (d, CH_2CH_2), 58.34 (s, CH_3O), 65.10 (m, OCH_2) 119 (m, TFSI) ^{31}P ($CDCl_3$, ppm) δ: 44.95 $^{19}F\{^1H\}$ ($CDCl_3$, ppm) δ: -79.9

Tricyclohexyl(2-methoxyethyl)phosphonium bis(trifluoromethylsulfonyl)imide (P_{Cy201}-TFSI)

3.0 g of P_{Cy201}-Br and 2.14 g of LiTFSI were combined in water and stirred for several hours. Dichloromethane (10 mL) was added and the aqueous layer was removed. The organic layer was washed repeatedly with deionized water until the extract showed no visible precipitation with $AgNO_3$. The DCM was then removed under vacuum and the ionic liquid was dried at vacuum at 100°C overnight. Yield: 4.36 g (92%) ^1H ($CDCl_3$, ppm) δ: 1.33-1.95 (m, 33H, Cy), 2.50-2.73 (m, 5H, *CH*Cy, PCH_2), 3.28 (s, 3H,

CH_3O), 3.69 (m, 2H, OCH_2) $^{13}C\{^1H\}$ ($CDCl_3$, ppm) δ: 25.71 (d, PCH_2CH_2), 26.65 (d, PCH_2CH_2), 29.93 (d, PCHCy), 39.7-41.1 (Cy), 58.79 (s, CH_3O), 65.54 (m, OCH_2) 119 (m, TFSI) ^{31}P ($CDCl_3$, ppm) δ: 26.12 $^{19}F\{^1H\}$ ($CDCl_3$, ppm) δ: -79.9

Synthesis of BF_4 ionic liquids

Triethyl(2-methoxyethyl)phosphonium tetrafluoroborate (P_{201}-BF_4)

4.28 g of P_{201}-Br and 1.82 g of $NaBF_4$ were combined in water and stirred for several hours. Acetone (10 mL) was added and the aqueous layer was removed. $AgBF_4$ was then added to the organic layer until no precipitation of AgBr was seen. The solution was filtered, if needed, and the acetone was then removed under vacuum and the ionic liquid was dried at vacuum at 100℃ until no residual water or acetone was seen by NMR. Yield: 3.55 g (81%) ^1H (DMSO, ppm) δ: 1.12 (m, 9H, CH_2CH_3), 2.19 (m, 6H, CH_2CH_3), 2.50 (m, 2H, CH_2CH_2), 3.22 (s, 3H, CH_3O), 3.60 (m, 2H, OCH_2) $^{13}C\{^1H\}$ (DMSO, ppm) δ: 5.49 (CH_2CH_3), 12.65 (CH_2CH_3), 19.14 (CH_2CH_2), 59.07 (CH_3O), 65.10 (OCH_2) ^{31}P (DMSO, ppm) δ: 40.13 $^{19}F\{^1H\}$ (DMSO, ppm) δ: -148.8

Triethyl(1H,1H,2H,2H-perfluorohexyl)phosphonium tetrafluoroborate (P_{2F4}-BF_4)

1.25 g of P_{2F4}-I and 0.38 g of $NaBF_4$ were combined in water and stirred for several hours. Acetone (10 mL) was added and the aqueous layer was removed. $AgBF_4$ was then added to the organic layer until no precipitation of AgI was seen. The solution was filtered, if needed, and the acetone was then removed under vacuum and the ionic liquid was dried at vacuum at 100℃ until no residual water or acetone was seen by NMR. Yield: 1.12 g (73%) ^1H (DMSO, ppm) δ: 1.32 (m, 9H, CH_2CH_3), 2.30-2.53 (b, 10H, CH_2), $^{13}C\{^1H\}$ (DMSO, ppm) δ: 5.82 (CH_2CH_3), 12.55 (d, CH_2CH_3), 19.34 (d,

P*CH*$_2$CH$_2$), 24.14 (s, PCH$_2$*CH*$_2$) ^{31}P (DMSO, ppm) δ: 40.97 ^{19}F{^{1}H} δ: -81.50 (3F), -115.02 (2F), -123.86 (2F), -126.43 (2F), -148.8 (BF_4)

Triethyl(2-ethyl-3,5-dioxolane)phosphonium tetrafluoroborate (P_{Diox}-BF_4)

1.5 g of P_{Diox}-Br and 0.563 g of $NaBF_4$ were combined in water and stirred for several hours. Acetone (10 mL) was added and the aqueous layer was removed. $AgBF_4$ was then added to the organic layer until no precipitation of AgBr was seen. The solution was filtered, if needed, and the acetone was then removed under vacuum and the ionic liquid was dried at vacuum at 100℃ until no residual water or acetone was seen by NMR. Yield: 0.85 g (54%) ^{1}H (DMSO, ppm) δ: 1.22 (m, 9H, CH$_2$*CH*$_3$), 1.92 (m, 2H, CH*CH*$_2$), 2.19 (m, 8H, P*CH*$_2$), 3.83 (m, 4H, CH$_2$O), 4.93 (m, 1H, O*CH*CH$_2$) ^{13}C{^{1}H} (DMSO, ppm) δ: 5.49 (CH$_2$*CH*$_3$), 12.25 (d, *CH*$_2$CH$_3$), 24.94 (s, OCH*CH*$_2$), 64.71 (s, CH$_2$O), 101.36 (d, O*CH*CH$_2$) ^{31}P (DMSO, ppm) δ: 40.66 ^{19}F{^{1}H} (DMSO, ppm) δ: -148.8

Di-tert-butylmethyl(2-methoxyethyl)phosphonium tetrafluoroborate ($P_{TTMe201}$-BF_4)

1.46 g of $P_{TTMe201}$-Br and 0.53 g of $NaBF_4$ were combined in water and stirred for several hours. Acetone (10 mL) was added and the aqueous layer was removed. $AgBF_4$ was then added to the organic layer until no precipitation of AgBr was seen. The solution was filtered, if needed, and the acetone was then removed under vacuum and the ionic liquid was dried at vacuum at 100℃ until no residual water or acetone was seen by NMR. Yield: 1.22 g (81%) ^{1}H (DMSO, ppm) δ: 1.45 (d, 18H, CCH$_3$), 1.85 (d, 3H, PCH$_3$), 2.45 (m, 2H, *CH*$_2$CH$_2$), 3.35 (s, 3H, CH$_3$O), 3.75 (m, 2H, OCH$_2$) ^{13}C{^{1}H} (DMSO, ppm) δ: 13.52 (PCH$_3$), 33.09 (d, C*CH*$_3$), 18.01 (d, *CH*$_2$CH$_2$),

58.19 (s, CH_3O), 65.68 (m, OCH_2) ^{31}P (DMSO, ppm) δ: 48.63 $^{19}F\{^1H\}$ (DMSO, ppm) δ: -148.8

Dimethylphenyl(2-methoxyethyl)phosphonium tetrafluoroborate ($P_{MePh201}$-BF_4)

2.0 g of $P_{MePh201}$-Br and 0.80 g of $NaBF_4$ were combined in water and stirred for several hours. Acetone (10 mL) was added and the aqueous layer was removed. $AgBF_4$ was then added to the organic layer until no precipitation of AgBr was seen. The solution was filtered, if needed, and the acetone was then removed under vacuum and the ionic liquid was dried at vacuum at 100℃ until no residual water or acetone was seen by NMR. Yield: 1.62 g (78%) ^1H (DMSO, ppm) δ: 2.18 (d, 6H, PCH_3), 2.76 (m, 2H, CH_2CH_2), 3.21 (s, 3H, CH_3O), 3.65 (m, 2H, OCH_2), 7.55 (m, 3H, Ar-H), 7.97 (m, 2H, Ar-H) $^{13}C\{^1H\}$ (DMSO, ppm) δ: 10.02 (PCH_3), 25.71 (d, CH_2CH_2), 59.02 (s, CH_3O), 65.97 (m, OCH_2), 120.99, 129.97, 131.82, 134. 38 (Ar) ^{31}P (DMSO, ppm) δ: 25.73$^{19}F\{^1H\}$ (DMSO, ppm) δ: -148.8

Dimethylphenylpentylphosphonium tetrafluoroborate (P_{MePh5}-BF_4)

1.95 g of P_{MePh5}-Br and 0.74 g of $NaBF_4$ were combined in water and stirred for several hours. Acetone (10 mL) was added and the aqueous layer was removed. $AgBF_4$ was then added to the organic layer until no precipitation of AgBr was seen. The solution was filtered, if needed, and the acetone was then removed under vacuum and the ionic liquid was dried at vacuum at 100℃ until no residual water or acetone was seen by NMR. Yield: 1.36 g (68%) ^1H (DMSO, ppm) δ: 0.71 (d, 3H, CH_3CH_2), 1.10-1.43 (m, 6H, pentyl CH_2), 2.45 (d, 6H, PCH_3), 2.87 (m, 2H, PCH_2CH_2), 7.55 (m, 3H, Ar-H), 7.97 (m, 2H, Ar-H) $^{13}C\{^1H\}$ (DMSO, ppm) δ: 5.61 (pentyl CH_3),

8.12 (PCH_3), 13.17 (s, CH_3CH_2), 17.15 ($CH_2CH_2CH_2$) 21.25 (d, PCH_2CH_2), 23.19 (d, PCH_2CH_2), 120.99, 129.97, 131.82, 134. 38 (Ar) ^{31}P (DMSO, ppm) δ: 26.12 $^{19}F\{^1H\}$ (DMSO, ppm) δ: -148.8

Tri-iso-butyl(2-methoxyethyl)phosphonium tetrafluoroborate (P_{iPr201}-BF_4)

1.09 g of P_{iPr201}-Br and 0.418 g of $NaBF_4$ were combined in water and stirred for several hours. Acetone (10 mL) was added and the aqueous layer was removed. $AgBF_4$ was then added to the organic layer until no precipitation of AgBr was seen. The solution was filtered, if needed, and the acetone was then removed under vacuum and the ionic liquid was dried at vacuum at 100℃ until no residual water or acetone was seen by NMR. Yield: 0.75 g (64%) ^1H (DMSO, ppm) δ: 1.10 (m, 18H, $CHCH_3$), 2.50-2.69 (m, 5H, $CHCH_3$, PCH_2), 3.05 (s, 3H, CH_3O), 3.47 (m, 2H, OCH_2) $^{13}C\{^1H\}$ (DMSO, ppm) δ: 16.40 ($CHCH_3$), 20.47 (d, $CHCH_3$), 21.03 (d, CH_2CH_2), 58.34 (s, CH_3O), 65.10 (m, OCH_2) ^{31}P (DMSO, ppm) δ: 44.95 $^{19}F\{^1H\}$ (DMSO, ppm) δ: -148.8

Tricyclohexyl(2-methoxyethyl)phosphonium tetrafluoroborate (P_{Cy201}-BF_4)

1.3 g of P_{Cy201}-Br and 0.34 g of $NaBF_4$ were combined in water and stirred for several hours. Acetone (10 mL) was added and the aqueous layer was removed. $AgBF_4$ was then added to the organic layer until no precipitation of AgBr was seen. The solution was filtered, if needed, and the acetone was then removed under vacuum and the ionic liquid was dried at vacuum at 100℃ until no residual water or acetone was seen by NMR. Yield: 0.75 g (57%) ^1H (DMSO, ppm) δ: 1.33-1.95 (m, 33H, Cy), 2.50-2.73 (m, 5H, $CHCy$, PCH_2), 3.28 (s, 3H, CH_3O), 3.69 (m, 2H, OCH_2) $^{13}C\{^1H\}$ (DMSO, ppm) δ:

25.71 (d, $PCH_2\mathit{CH_2}$), 26.65 (d, $P\mathit{CH_2}CH_2$), 29.93 (d, P*CH*Cy), 39.7-41.1 (Cy), 58.79 (s, CH_3O), 65.54 (m, OCH_2) ^{31}P (DMSO, ppm) δ: 26.12 $^{19}F\{^1H\}$ (DMSO, ppm) δ: -148.8

Synthesis of PF_6 ionic liquids

Triethyl(2-methoxyethyl)phosphonium hexafluorophosphate (P_{201}-PF_6)

1.59 g of P_{201}-Br and 1.04 g of $NaPF_6$ were combined in water and stirred for several hours. DCM (10 mL) was added and the aqueous layer was removed. $AgPF_6$ was then added to the organic layer until no precipitation of AgBr was seen. The solution was filtered, if needed, and the DCM was then removed under vacuum and the ionic liquid was dried at vacuum at 100℃ until no residual water or DCM was seen by NMR. Yield: 1.24 g (62%) ^1H ($CDCl_3$, ppm) δ: 1.12 (m, 9H, $CH_2\mathit{CH_3}$), 2.19 (m, 6H, $\mathit{CH_2}CH_3$), 2.50 (m, 2H, $\mathit{CH_2}CH_2$), 3.22 (s, 3H, CH_3O), 3.60 (m, 2H, OCH_2) $^{13}C\{^1H\}$ ($CDCl_3$, ppm) δ: 5.49 ($CH_2\mathit{CH_3}$), 12.65 ($\mathit{CH_2}CH_3$), 19.14 ($\mathit{CH_2}CH_2$), 59.07 (CH_3O), 65.10 (OCH_2) ^{31}P ($CDCl_3$, ppm) δ: 40.13 $^{19}F\{^1H\}$ ($CDCl_3$, ppm) δ: -70.52 (d)

Triethyl(1H,1H,2H,2H-perfluorohexyl)phosphonium hexafluorophosphate (P_{2F4}-PF_6)

0.75 g of P_{2F4}-I and 0.26 g of $NaPF_6$ were combined in water and stirred for several hours. DCM (10 mL) was added and the aqueous layer was removed. $AgPF_6$ was then added to the organic layer until no precipitation of AgI was seen. The solution was filtered, if needed, and the DCM was then removed under vacuum and the ionic liquid was dried at vacuum at 100℃ until no residual water or DCM was seen by NMR. Yield: 0.44 g (55%) ^1H ($CDCl_3$, ppm) δ: 1.32 (m, 9H, $CH_2\mathit{CH_3}$), 2.30-2.53 (b, 10H, CH_2), $^{13}C\{^1H\}$ ($CDCl_3$, ppm) δ: 5.82 ($CH_2\mathit{CH_3}$), 12.55 (d, $\mathit{CH_2}CH_3$), 19.34 (d, $P\mathit{CH_2}CH_2$), 24.14 (s, $PCH_2\mathit{CH_2}$) ^{31}P ($CDCl_3$, ppm) δ: 40.97 $^{19}F\{^1H\}$ δ: -81.50 (3F), -115.02 (2F), -123.86 (2F), -126.43 (2F), -70.52 (d)

Triethyl(2-ethyl-3,5-dioxolane)phosphonium hexafluorophosphate (P_{Diox}-PF_6)

1.0 g of P_{Diox}-Br and 0.55 g of $NaPF_6$ were combined in water and stirred for several hours. DCM (10 mL) was added and the aqueous layer was removed. $AgPF_6$ was then added to the organic layer until no precipitation of AgBr was seen. The solution was filtered, if needed, and the DCM was then removed under vacuum and the ionic liquid was dried at vacuum at 100℃ until no residual water or DCM was seen by NMR. Yield: 0.54 g (45%) ^{1}H ($CDCl_3$, ppm) δ: 1.22 (m, 9H, CH_2CH_3), 1.92 (m, 2H, $CHCH_2$), 2.19 (m, 8H, PCH_2), 3.83 (m, 4H, CH_2O), 4.93 (m, 1H, $OCHCH_2$) ^{13}C{^{1}H} ($CDCl_3$, ppm) δ: 5.49 (CH_2CH_3), 12.25 (d, CH_2CH_3), 24.94 (s, $OCHCH_2$), 64.71 (s, CH_2O), 101.36 (d, $OCHCH_2$) ^{31}P ($CDCl_3$, ppm) δ: 40.66 ^{19}F{^{1}H} (CDCL3, ppm) δ: -70.52 (d)

Di-tert-butylmethyl(2-methoxyethyl)phosphonium hexafluorophosphate ($P_{TTMe201}$-PF_6)

0.54 g of $P_{TTMe201}$-Br and 0.31 g of $NaPF_6$ were combined in water and stirred for several hours. DCM (10 mL) was added and the aqueous layer was removed. $AgPF_6$ was then added to the organic layer until no precipitation of AgBr was seen. The solution was filtered, if needed, and the DCM was then removed under vacuum and the ionic liquid was dried at vacuum at 100℃ until no residual water or DCM was seen by NMR. Yield: 0.45 g (68%) ^{1}H ($CDCl_3$, ppm) δ: 1.45 (d, 18H, CCH_3), 1.85 (d, 3H, PCH_3), 2.45 (m, 2H, CH_2CH_2), 3.35 (s, 3H, CH_3O), 3.75 (m, 2H, OCH_2) ^{13}C{^{1}H} ($CDCl_3$, ppm) δ: 13.52 (PCH_3), 33.09 (d, CCH_3), 18.01 (d, CH_2CH_2), 58.19 (s, CH_3O), 65.68 (m, OCH_2) ^{31}P ($CDCl_3$, ppm) δ: 48.63 ^{19}F{^{1}H} ($CDCl_3$, ppm) δ: -70.52 (d)

Dimethylphenyl(2-methoxyethyl)phosphonium hexafluorophosphate ($P_{MePh201}$-PF_6)

1.62 g of $P_{MePh201}$-Br and 0.97 g of $NaPF_6$ were combined in water and stirred for several hours. DCM (10 mL) was added and the aqueous layer was removed. $AgPF_6$ was then added to the organic layer until no precipitation of AgBr was seen. The solution was filtered, if needed, and the DCM was then removed under vacuum and the ionic liquid was dried at vacuum at 100°C until no residual water or DCM was seen by NMR. Yield: 1.48 g (74%) ^{1}H ($CDCl_3$, ppm) δ: 2.18 (d, 6H, PCH_3), 2.76 (m, 2H, CH_2CH_2), 3.21 (s, 3H, CH_3O), 3.65 (m, 2H, OCH_2), 7.55 (m, 3H, Ar-H), 7.97 (m, 2H, Ar-H) ^{13}C{^{1}H} ($CDCl_3$, ppm) δ: 10.02 (PCH_3), 25.71 (d, CH_2CH_2), 59.02 (s, CH_3O), 65.97 (m, OCH_2), 120.99, 129.97, 131.82, 134. 38 (Ar) ^{31}P ($CDCl_3$, ppm) δ: 25.73^{19}F{^{1}H} ($CDCl_3$, ppm) δ: -70.52 (d)

Dimethylphenylpentylphosphonium hexafluorophosphate (P_{MePh5}-PF_6)

1.95 g of P_{MePh5}-Br and 1.12 g of $NaPF_6$ were combined in water and stirred for several hours. DCM (10 mL) was added and the aqueous layer was removed. $AgPF_6$ was then added to the organic layer until no precipitation of AgBr was seen. The solution was filtered, if needed, and the DCM was then removed under vacuum and the ionic liquid was dried at vacuum at 100°C until no residual water or DCM was seen by NMR. Yield: 1.86 g (78%) ^{1}H ($CDCl_3$, ppm) δ: 0.71 (d, 3H, CH_3CH_2), 1.10-1.43 (m, 6H, pentyl CH_2), 2.45 (d, 6H, PCH_3), 2.87 (m, 2H, PCH_2CH_2), 7.55 (m, 3H, Ar-H), 7.97 (m, 2H, Ar-H) ^{13}C{^{1}H} ($CDCl_3$, ppm) δ: 5.61 (pentyl CH_3), 8.12 (PCH_3), 13.17 (s, CH_3CH_2), 17.15 ($CH_2CH_2CH_2$) 21.25 (d, PCH_2CH_2), 23.19 (d, PCH_2CH_2), 120.99, 129.97, 131.82, 134. 38 (Ar) ^{31}P ($CDCl_3$, ppm) δ: 26.12 ^{19}F{^{1}H} ($CDCl_3$, ppm) δ: -70.52 (d)

Tri-iso-butyl(2-methoxyethyl)phosphonium hexafluorophosphate (P_{iPr201}-PF_6)

1.05 g of P_{iPr201}-Br and 0.590 g of $NaPF_6$ were combined in water and stirred for several hours. DCM (10 mL) was added and the aqueous layer was removed. $AgPF_6$ was then added to the organic layer until no precipitation of AgBr was seen. The solution was filtered, if needed, and the DCM was then removed under vacuum and the ionic liquid was dried at vacuum at 100°C until no residual water or DCM was seen by NMR. Yield: 0.81 g (63%) ^{1}H ($CDCl_3$, ppm) δ: 1.10 (m, 18H, CH*CH*$_3$), 2.50-2.69 (m, 5H, *CH*CH_3, PCH_2), 3.05 (s, 3H, CH_3O), 3.47 (m, 2H, OCH_2) ^{13}C{^{1}H} ($CDCl_3$, ppm) δ: 16.40 (CH*CH*$_3$), 20.47 (d, *CH*CH_3), 21.03 (d, CH_2CH_2), 58.34 (s, CH_3O), 65.10 (m, OCH_2) ^{31}P ($CDCl_3$, ppm) δ: 44.95 ^{19}F{^{1}H} ($CDCl_3$, ppm) δ: -70.52 (d)

Tricyclohexyl(2-methoxyethyl)phosphonium hexafluorophosphate (P_{Cy201}-PF_6)

1.02 g of P_{Cy201}-Br and 0.416 g of $NaPF_6$ were combined in water and stirred for several hours. DCM (10 mL) was added and the aqueous layer was removed. $AgPF_6$ was then added to the organic layer until no precipitation of AgBr was seen. The solution was filtered, if needed, and the DCM was then removed under vacuum and the ionic liquid was dried at vacuum at 100°C until no residual water or DCM was seen by NMR. Yield: 0.92 g (65%) ^{1}H ($CDCl_3$, ppm) δ: 1.33-1.95 (m, 33H, Cy), 2.50-2.73 (m, 5H, *CH*Cy, PCH_2), 3.28 (s, 3H, CH_3O), 3.69 (m, 2H, OCH_2) ^{13}C{^{1}H} ($CDCl_3$, ppm) δ: 25.71 (d, PCH_2*CH_2*), 26.65 (d, P*CH_2*CH_2), 29.93 (d, P*CH*Cy), 39.7-41.1 (Cy), 58.79 (s, CH_3O), 65.54 (m, OCH_2) ^{31}P ($CDCl_3$, ppm) δ: 26.12 ^{19}F{^{1}H} ($CDCl_3$, ppm) δ: -70.52 (d)

Chapter 2: Efforts Toward the Synthesis of Ammonium and Phosphonium Ionic Liquids for the Capture of Carbon Dioxide

INTRODUCTION

During the past fifteen years there has been a proliferation of ionic liquid related studies across many different areas of chemistry. Early work was focused on the properties of many "base" ionic liquids, such as 1-ethyl-2-methylimidizolium salts, and their pertinence in unmodified forms for many applications. Subsequently, theoretical frameworks were established and further synthetic experience permitted the fine tuning of the physical properties of ionic liquids. As the field continued to mature, it was realized that the tunability of ionic liquids is not limited to only the physical and electrochemical properties. By deliberate synthetic design, ionic liquids can now act as scaffolds for desired chemical functionalities. Thus, a new concept referred to as task-specific ionic liquids (TSILs) was created. Though there is no single definition of a task-specific IL, the term is usually reserved for systems in which the ionic liquid functions in a role beyond that of a solvent.

One of the most attractive uses of TSILs is focused on catalysis. Most catalytic processes occur under either homogenous or heterogenous conditions, both of which have their advantages and disadvantages. In theory, an ionic liquid that functions as both a solvent and a catalyst can combine the advantages of both processes. If the substrate were in the same phase (i.e. dissolved in the ionic liquid), the selectivity and speed that is typically observed for homogenous catalysis can be achieved. Furthermore, due to the low volatilities of ionic liquids as a class, the resulting products could be easily separated through distillation or extraction, which represents a clear advantage typically observed for heterogenous catalysis. In 2002, Cole et al. reported a simple task-specific IL based on phosphonium sulfonates used for acid-catalyzed reactions.[56] More recently, Yue et al.

used monoethanolammonium acetate for the base-catalyzed Knoevenagel condensation of aryl aldehydes and ethyl cyanoacetate.[57] While there are more advanced TSILs that serve as ligands for metal-catalyzed reactions, it seems clear that simple modifications of IL chemistry could lead to significant results.

Although not by design, conventional ionic liquids long ago attracted interest in terms of gas absorption applications. Permanently polar gasses such as ammonia and sulfur dioxide, in addition to polarizable unsaturated alkenes such as ethylene or even benzene, typically have strong interactions with ionic liquids. Conversely, nonpolar gasses such as oxygen, nitrogen, and hydrogen sometimes exhibit less solubility in ionic liquids than in organic solvents.[58] This physisorption effect is often enhanced by the presence of fluorine containing anions, which more easily induce polarization in the target gasses. Once the field of task-specific ILs began to expand, efforts shifted from enhanced physisorption toward the use of chemisorption for greater gas capacity. In 2008, Tempel et al. demonstrated the storage of the dangerous gasses BH_3 and PH_3 by complexation to BF_4^- and $Cu_2Cl_3^-$, respectively.[59] By taking advantage of the Lewis acidity and basicity of these gasses, the authors were able to design ionic liquids for safer storage of extremely flammable compounds. Other examples of the successful storage of toxic gasses include the capture of Hg(0) from post-combustion flue gas,[60] and the chemisorption of H_2S by an imidizolium carboxylate IL.[61]

While the foregoing examples illustrate the application range of TSILs for gasses, they are only representative of a small fraction thereof. The majority of TSILs employed for gas storage are typically used for industrially and environmentally significant compounds. In this context, many ionic liquids have been designed with carboxylate or phosphate substituents that react with SO_2 to remove the latter from flue gas.[61–65] This reaction most often proceeds via the formation of new sulfonate function groups.

Ammonia has also been targeted by TSILs, by reaction with acidic substituents.[66] However, the primary target has consistently been the largest anthropomorphically generated pollutant, namely carbon dioxide.

CO_2 Capture Technologies

One of the most serious political and scientific concerns of the 21st century is that of global climate change. While there is no single cause for the climate changes observed by atmospheric scientists, it has been found that carbon dioxide is the primary contributor. Due to the increased industrialization of both modern and developing nations, approximately 30 billion metric tons of CO_2 are released into the atmosphere each year.[67] In order to combat this problem, the United Nations Intergovernmental Panel on Climate Change (IPCC) has established a two-pronged approach: promote renewable energies to eliminate CO_2 production, and sequester or chemically modify the CO_2 produced so that it does not reach the atmosphere. Regarding the latter approach, several technologies with distinct advantages and disadvantages such as zeolites, metal-organic frameworks, and fixation exist. When considering CO_2 capture technologies, it is important to be aware of the key problems related to the methods of CO_2 production. Chief among these is the problem of scale. Since billions of tons of CO_2 are being produced each year, capture technologies must be economical to be effective at any scale that will make a significant impact. Furthermore, this economy should be enhanced by a degree of reusability such that CO_2 can be introduced, removed, and reintroduced without loss of functionality. In this, the energy needed to create, maintain, and operate a technology is often its key characteristic. Secondly, the technology should exhibit a preference for CO_2 over other gasses to achieve efficient separation. This selectivity may be especially important in a process that generates other useful products where

sequestration is not desired. Finally, the technology should be operable over a wide range of pressures. Whether from auto emissions or industrial flue gas, CO_2 is found in systems ranging from 1 to 30 bar and in various compositions therein. The best system should exhibit an appreciable performance even at low pressures.

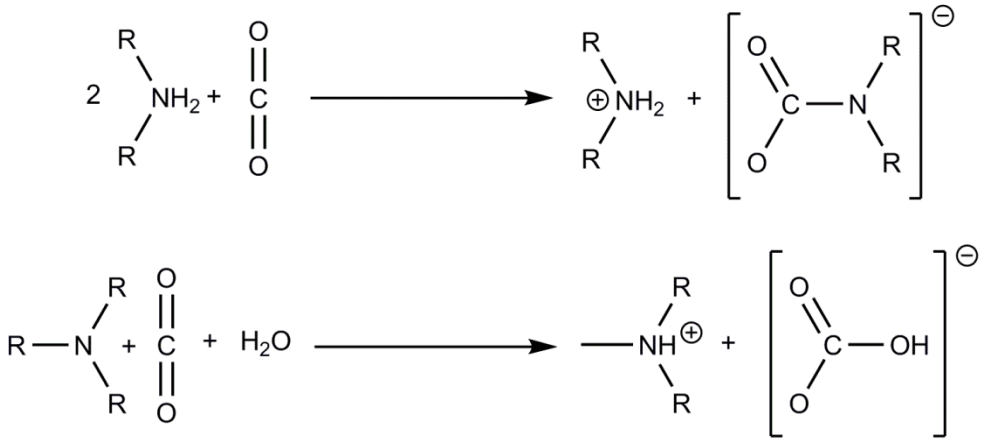

Scheme 2.1: CO_2 capture pathways for primary and secondary amines (top) which form ammonium carbamates or tertiary amines (bottom) which form ammonium carbonates.

The conventional "wet-scrubbing" of industrial gasses uses aqueous amine solutions (around 25-30 wt.%) for the chemical absorption of CO_2 through complexation to form carbamates (Scheme 2.1).[68] In the case of primary and secondary amines, carbon dioxide is absorbed in a 0.5:1 mol ratio (CO_2/amine), while tertiary amines absorb in a 1:1 ratio but exhibit much lower reactivity. This current method has two main advantages. The first is that small amines used for this, such as monoethanolamine (MEA), can be easily produced on a scale that is sufficiently large enough to impact the massive amounts of CO_2 produced each year. The wide variety of amines that can be used in this process also leads to a small degree of optimization of the reaction conditions. The second advantage is that after nearly 50 years of using these systems, the

engineering mechanisms and refinements are widely used and would not require extensive retrofitting, in contrast to new technologies which will bring their own engineering considerations. However, aqueous amine systems require elevated temperatures in the area of 100-140 ℃, due to the high heats of formation of the carbamate products. These temperatures greatly increase the energy needed for regeneration of the amine component and is magnified on the scale required for a global CO_2 solution.

Many solid adsorbants can also be used for carbon dioxide capture. Metal oxides represent the simplest and most earth-abundant solid systems. In these cases, compounds such as CaO can react at high temperatures (600-800 ℃) to form the corresponding carbonates, such as $CaCO_3$.[69] In this way, metal oxides can adsorb eqimolar amounts of CO_2 at temperatures at which other capture technologies would decompose. Unfortunately, even higher temperatures are needed for regeneration to the starting metal oxide, representing a substantial energy investment in order to maintain continuous operation. Furthermore, it has been demonstrated that regenerated oxides often do not reach their previous capacities due to structural rearrangements that reduce the porosity.[70]

Similar compounds such as zeolites, which are frameworks of aluminium and silicon oxides, do not follow the same chemisorption mechanism exhibited by CaO but can achieve useful capacities through physisorption. As a framework, zeolites have rigid, periodic pores that gas molecules can flow through and be trapped within by means of Van der Waals type interactions with the framework material. A high mark for zeolites was achieved in a NaY type structure in which CO_2 was adsorbed up to 5 mmol per gram of adsorbant (theoretical maximum of CaO = 17.8 mmol g^{-1}) at room temperature and a pressure of 0.1 bar.[71] However, this interaction is not particularly selective and is affected

by the polarizability. Nevertheless, the framework structure of zeolites often gives them a degree of size (or volume) selectivity. In this way, the pore size could be used to exclude many gasses other than CO_2, which would in effect increase the capacity of the material. However, competition from water can often be a problem in zeolites due to the physical space that is occupied and occasional occurrences of strong coordination to cationic species that are often incorporated into the framework. Since carbon dioxide and water are both products of combustion, there is often a significant amount of water vapor present in the gas stream. Furthermore, the resulting zeolites containing coordinated water molecules may require more intensive processes (i.e. T ≈ 300 ℃) for full regeneration.[72]

Somewhat analogous to zeolites, metal-organic frameworks (MOFs) feature rigid organic molecules linked together through coordination to a metal node. MOFs can provide a wide array of pore shapes, pore sizes, and crystal arrangements through modification of either the organic linker or the metal coordination site. In comparison with zeolites, MOFs typically possess greater internal surface areas (up to 5000 $m^2\ g^{-1}$) and high void volumes (55-90%).[73] This internal surface area allows for a much greater amount of gas adsorption via physisorption. As an example, a framework of Cr octahedra linked together by terphtalate molecules (MIL-101) exhibited CO_2 adsorption up to 40 mmol g^{-1} at high pressures.[74] The extent of interaction between the MOF and carbon dioxide can also be enhanced by inclusion of metal-coordinated ancillary ligands[75,76] or open metal sites.[77,78] Additionally, chemisorption can be introduced by use of amine functionalized metal ligands or organic linkers. For example, in 2008, Arstad et al. demonstrated a 4 wt% increase in CO_2 adsorption in two MOF structures when amines were grafted onto benzenedicarboxylate linkers,[76] while McDonald et al. reported a 3.5-fold increase in gravimetric capacity when metal binding ethylenediamine ligands were

introduced.[79] MOFs typically excel at very high pressures (> 30 bar) that are used in pre-combustion systems. However, like other solid systems, MOFs have disadvantages in the context of gas adsorption applications. The periodic crystallinity that gives these compounds excellent thermal stability can also result in slower uptake times than liquid counterparts.[80] In turn, this can lead to prolonged regeneration times du to the fact that the CO_2 must be evacuated from the highly porous structure. Furthermore, secondary engineering concerns such as mechanical strength and thermal conductivity must be taken into consideration when a solid is used as an adsorbant.

Task-Specific Ionic Liquids for CO_2 Capture

As stated earlier, ionic liquids have long been targeted for their favorable gas absorption properties. For CO_2 applications, ionic liquids possess several distinct advantages. For example, ILs can more easily be incorporated into current gas stream processes than solid materials like MOFs or zeolites, possibly making them more economical from an engineering perspective. Due to being largely non-volatile, ILs will not be subject to losses due to vaporization into the gas stream or the environment. Additionally, the high thermal stabilities exhibited by most ILs (upwards of 300 ℃) allow them to function in most processes. Based solely on physisorption, most ionic liquids can absorb up to 0.2 mol of CO_2 per mole of IL at low pressure (ca. 1 bar) and the absorption increases almost linearly at higher pressures.[81] Generally, greater fluorination and longer alkyl chain length increases CO_2 capacity due to greater Lewis acid-base interactions and more free volume between molecules, respectively.[82] Despite the innate advantages of ionic liquids, they are not very competitive in capacity when compared to porous solids like MOFs when relying on physisorption mechanisms alone.

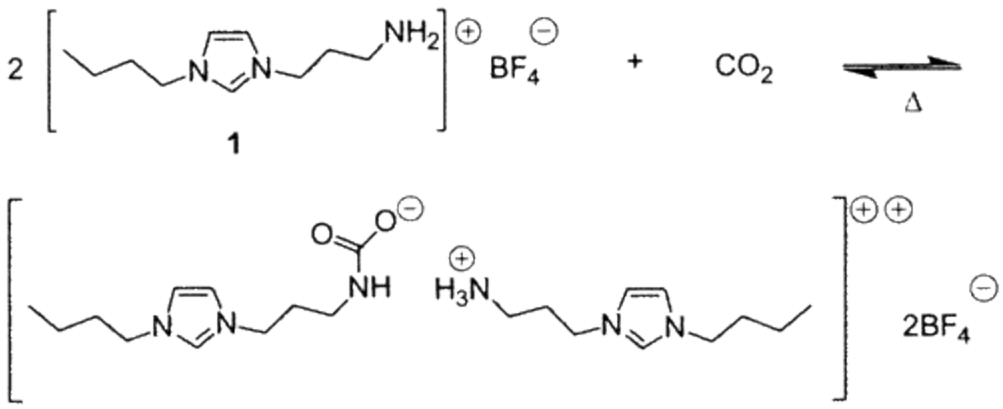

Figure 2.1: Proposed mechanism of CO_2 absorption by an amine-functionalized imidizolium ionic liquid synthesized by Davis et al.[83]

In 2002, Davis and coworkers at the University of Southern Alabama synthesized a new amine-functionalized imidizolium ionic liquid. Using the same chemisorption method (Figure 2.1) as seen in aqueous amine solutions, the authors reported absorbtion up to 0.5 mol of CO_2 per mol of IL after 3 hours.[83] Additionally, this TSIL only had to be heated to 80-100 ℃ for complete regeneration which is an appreciably lower temperature than the those needed for aqueous amine solutions. The most significant drawback seen in this work was an increase in viscosity upon addition of CO_2. With the formation of new carbamate and ammonium ions upon complexation, strong new ion-ion and hydrogen bonding interactions are made which account for this dramatic increase is viscosity.[84] Following this report, several other cation-based systems were developed, each using the tunability to enhance the physical properties of the ionic liquids while leaving the CO_2 capacity basically unchanged. More recently, however, Zhang et al. prepared an imidizolium cation with two amine functionalities that was able to capture 1 mol of CO_2 per mole of cation.[85]

In the other half of the ionic liquid, anions underwent a significant growth in diversity since amine functionality is easily grafted onto carboxylates. Some of the most popular of these anions include natural amino acids and derivatives thereof. While these amino acid ionic liquids suffer from reduced thermal stability, the presence of separate amine functionalities greatly increases the capacity for CO_2 capture. For instance, a phosphonium ionic liquid with an amine functionalized cation in addition to an amino acid anion has been shown to be capable of absorbing 1 mole of CO_2 per mole of ionic liquid, doubling the capacity of most cation-only systems.[86] Additionally, some amino acids have been observed absorbing more CO_2 than would be suggested by the 1:2 ratio described in Scheme 2.1. In these cases, it is postulated that carbon dioxide combines with the amine to make an ammonium carboxylate zwitterion (Scheme 2.2).

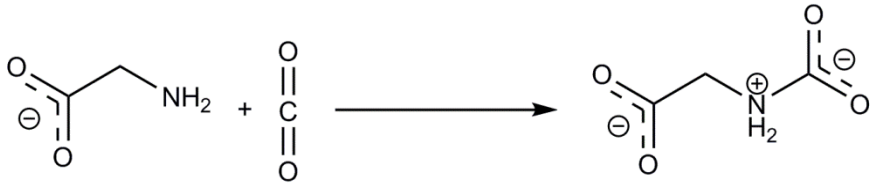

Scheme 2.2: Simplified example of the proposed mechanism of equimolar CO_2 absorption seen in some amino acids.

In such a model, an amino acid would be able to absorb one mole of CO_2 per mole of anion. In practice, however, no evidence has been seen of total use of this mechanism; the anions capable of this mechanism most often use some mixture of the 1:2 and 1:1 pathways.[85,87] Surprisingly, ionic liquids based on amino acids show low glass transition temperatures below 0 °C, despite the fact that carboxylates are relatively "strong" anions with larger lattice energies. Following the observation of this 1:1 pathway, other, more exotic anions such as triazolates and tetrazolates were considered. In triazolates used for SO_2 capture, the 1:1 mechanism has been refined to 1 mole of SO_2

per mole of N atoms. As such, triazolate has been seen to absorb up to 3 moles of SO_2 by itself, and tetrazolate up to four moles.[88] Theoretical calculations reveal that this behavior may not be seen in carbon dioxide due to the energy cost involved in changing its linear geometry, but more elevated temperatures and pressures may overcome this barrier.[89] While azolate anions are prone to serious stability problems, they do illustrate that the capacity for carbon dioxide in ionic liquids could be increased by careful design and is only limited by concerns about the physical properties.

As stated earlier, the chief drawback of ionic liquids as absorbents is viscosity. In liquids, high viscosity lowers the rate of mass and heat diffusion and can lead to inhomogenous reaction conditions and thermal hot spots. Additionally, high viscosity increases the amount of mechanical energy needed to efficiently pump the liquid. The viscosity of aqueous amine solutions used currently is around 10 cP, and depends on the exact amount of amine in solution. In contrast, the least viscous ionic liquid available, task-specific or not, is approximately twice this value. In terms of task-specific ILs for carbon dioxide capture, the comparison is worse. Typical TSILs for this application have viscosities at least an order of magnitude higher than aqueous amine solutions, with many being two orders of magnitude higher. Additionally, viscosity tends to increase upon complexation of CO_2. One of the simplest ways to counteract this effect is seen in the amino acid proline. Due to its ring structure, the amine of proline is secondary instead of primary which in turn leads to less hydrogens being available for hydrogen bonding.[84] In TSILs that use prolate anions, very little increase in viscosity is seen upon addition of carbon dioxide.[90] In this way, modification of primary amines to secondary may result in better physical properties. The second way to counteract the high viscosity is through addition of another solvent. Small amount of organic solvents as dilutants have been shown to have a significant effect on viscosity. In addition, water has been shown to

lower viscosities in TSILs for carbon dioxide capture. The ionic liquid [P_{66614}][Pro] has a dry viscosity around 700 cP, but addition of only 0.1 wt% water decreases this viscosity by almost 100 cP.[91] Since most post-combustion flue gas already contains water vapor, a normally hydroscopic TSIL could absorb this water vapor and lower the viscosity without any addition of outside solvents. Following this line of reasoning, many systems are being developed that utilize TSIL solutions, analogous to aqueous amine solutions, to achieve the physical properties needed (namely, viscosity) with the high capacities available to ionic liquids.[92–94]

Research Objectives

With these results in mind, the primary objective was to apply these principles to novel phosphonium and ammonium ionic liquids. In regards to the key advantage of amine-functionalized TSILs, capture capacity, phosphonium and ammonium cations present a unique opportunity. "Baseline" imidizolium cations have two substituents that can be functionalized, while phosphonium and ammonium cations have four substituents available for functionalization. As such, a "fully loaded" –onium cation will have twice the capacity of an analogous imidizolium cation. Figure 2.2 depicts the target molecule that would be an example of a new class of task-specific ionic liquids.

In this design, each of the four substituents features one amine functionality, affording a theoretical capacity of 2 moles of CO_2 per mole of cation. If the anticipated pathway were to occur, it would represent a rare occurrence of intramolecular absorption, and would represent an interesting contrast to the 1:2 mechanism which usually occurs between amine functionalities on two different molecules. To counteract any viscosity issues that arise from intense hydrogen bonding networks, only secondary amines would be used that are located away from the periphery of the molecule where more ordered

hydrogen bonding can occur. Additionally, anion exchange of the halide could be carried out to introduce anions with greater capacities (such as amino acids) or to improve physical properties through anions such as TFSI. The present work describes the attempts that have been made to synthesize this and similar cations as carbon dioxide capture agents.

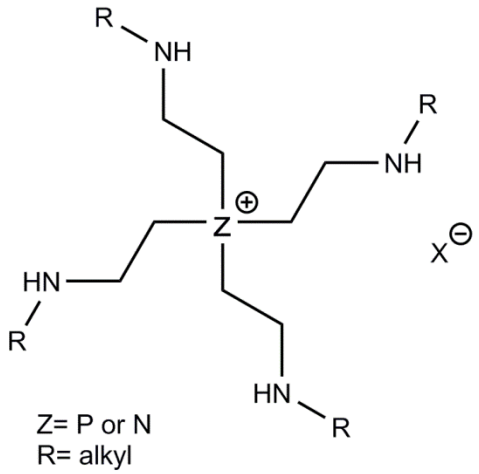

Figure 2.2: General structure of proposed new task-specific phosphonium and ammonium ionic liquids for carbon dioxide capture.

RESULTS AND DISCUSSION

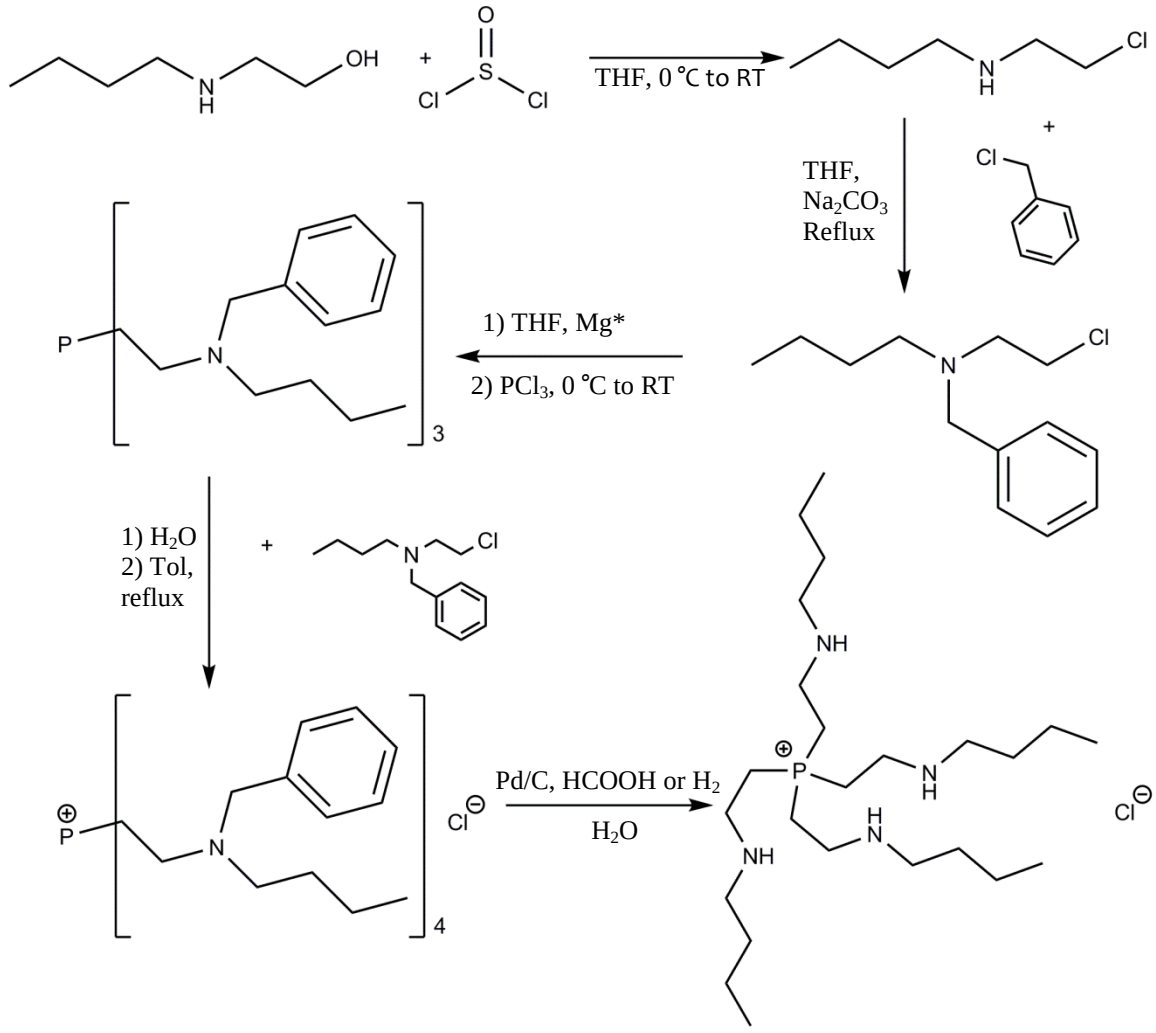

Scheme 2.3: Original synthetic scheme developed for the creation of the new phosphonium ionic liquids.

For the syntheses of these materials, several different methods were employed to append amines to phosphine precursors. In the originally devised route (Scheme 2.3), *N*-butyl, *N*-ethanolamine would undergo a chlorination by thionyl chloride to afford a halogenated amine which could subsequently be protected by a benzyl group. This product, in turn, could be added to activated magnesium to form a Grignard that could react with phorphorus trichloride to form a new triaminophosphine. This new phosphine

could then be refluxed with an equivalent of halogenated ammonium from the previous dehydrohalogenation to form a phosphonium chloride. The four amines on this proposed new phosphonium could then be deprotected via palladium-catalyzed hydrogenation with formic acid or, more crudely, by extended reflux in concentrated HCl. While this proposed scheme is very straightforward, it suffers from a number of key disadvantages. In the first chlorination step, sulfur dioxide would be the gaseous byproduct of successful reaction. In the course of making new materials for the capture of pollutant CO_2, it would be somewhat antithetical to produce four moles of the more toxic SO_2 in pursuit of this goal. Furthermore, the stability of the halogenated amine toward intermolecular amine alkylation may also be problematic at the elevated temperatures needed for efficient benzyl protection. In general, Grignard reagents are favored for the synthesis of alkyl and aryl phosphines of many types, however, Grignard reagents are air and moisture sensitive and reactions utilizing them are only moderately yielding at best (40-60%). In the formation of the phosphonium, careful control would have to be used to ensure that the phosphorus atom reacts preferentially over any nitrogen atom. Subsequent deprotection with formic acid would create four moles of carbon dioxide per cation, while reflux in concentrated acid could degrade the molecule. Furthermore, partial deprotection would result in a mixture of four different phosphonium cations with very similar chemistry that would be very difficult to separate. If such a mixture were used as-is, extensive tests would need to be done on a batch-by-batch basis to determine exactly how many deprotected and protected amines existed. This ratio of secondary and tertiary amines would greatly affect the theoretical CO_2 capacity. In light of these issues, new synthetic methods were investigated with a primary focus on pathways that produce 100% pure phosphonium salts in the final step.

Synthesis via Phosphine Gas

The first alternative path investigated involved the free radical addition of alkenes to phosphine gas, PH_3 (Scheme 2.4).

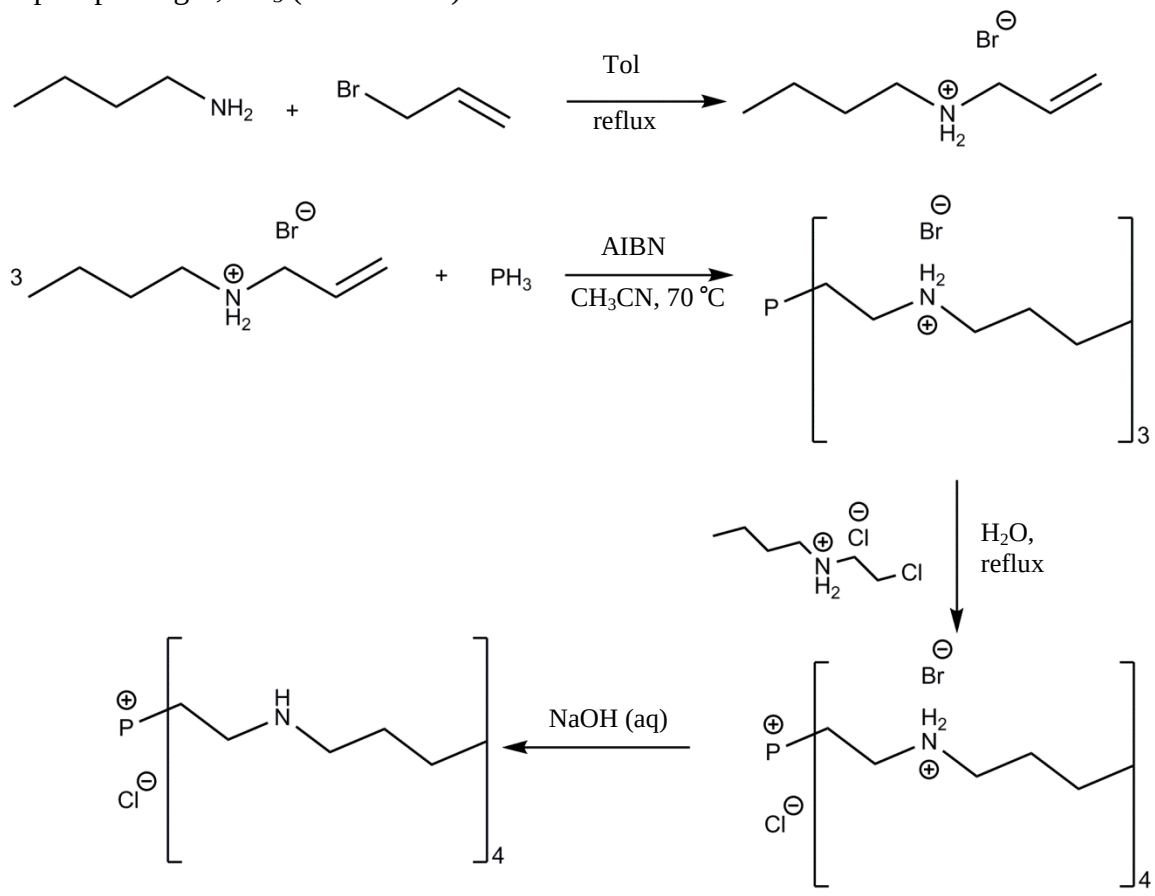

Scheme 2.4: Proposed synthetic route via free-radical addition of alkenes to phosphine gas.

As early as 1961, free radicals were being used for the addition of simple alkenes such as 1-octene to phosphine gas.[95] More recently, Gusarova et al. used this technique for the addition of vinyl thioethers in the creation of tris[(organylthio)-ethyl]phosphine oxides[96] In these reactions (Scheme 2.5), an organic radical such as α,α'-azobisisobutyronitrile (AIBN) abstracts a hydrogen atom from PH_3 thereby forming a phosphoryl radical (step 1). The latter radical then undergoes nucleophillic attack on one

of the sp^2 hybridized alkenyl carbons (step 2) to generate a new carbon radical which can abstract a hydrogen atom from either AIBN or a different phosphine molecule thereby terminating the chain (step 3). This process then continues until all of the phosphine has been fully alkylated, or until the alkene runs out.

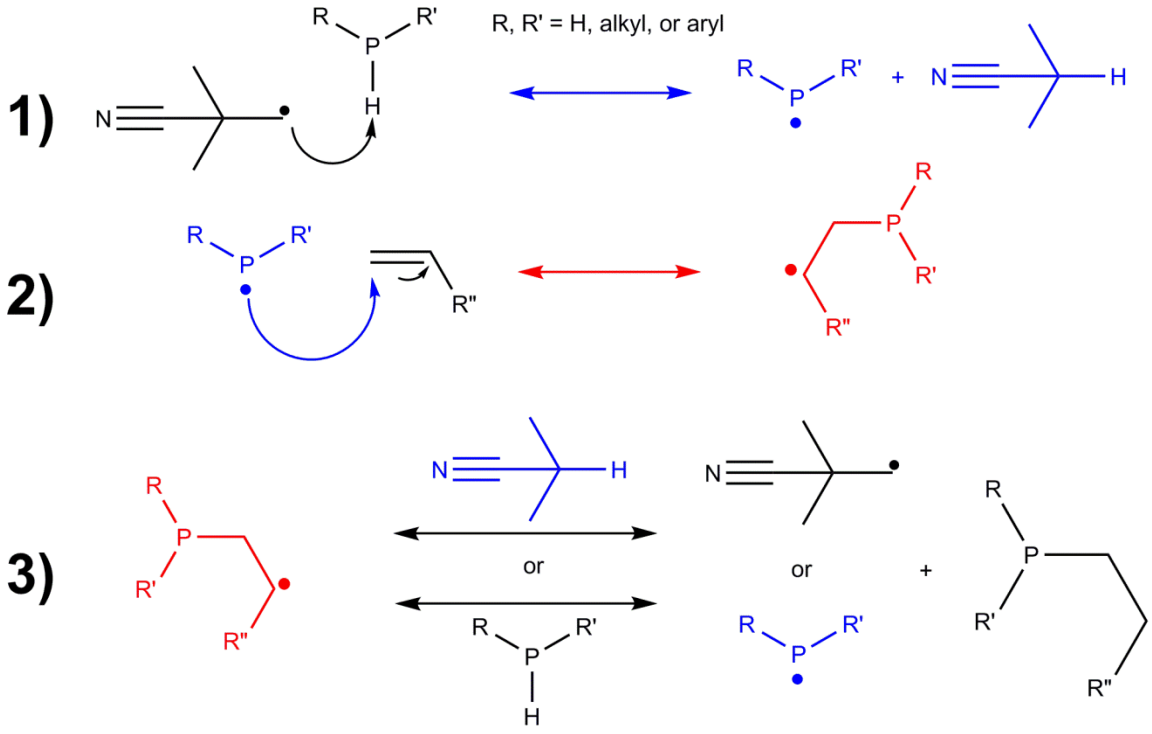

Scheme 2.5: Mechanism of the free radical addition of phosphine gas to alkenes initiated by an AIBN radical.

The primary advantage of this mechanism is that of atom-economy since there are no byproducts and every atom of the reactants ends in one product. However, by its nature, primary and secondary phosphines can also be produced if the reaction does not go to completion. The simplest way to control the ratio of products is to make phosphine gas the limiting reactant. Given enough time, this ensures that each phosphine will be fully alkylated, and excess alkene can be reused in further attempts.

In the present work, butylallylammonium bromide or butylallylamine were added to a solution of AIBN in acetonitrile or toluene, respectively, and heated under a phosphine atmosphere. After several hours, excess phosphine was purged from the reaction flask and replaced by dry nitrogen. A small aliquot of the reaction solution was used for ^{31}P NMR analysis to observe the progress of reaction. Initial studies used stoichiometric quantities of phosphine gas (approx 14 psi overpressure) and nitrogen at ambient pressure, but phosphorus NMR of solutions of the ammonium and amine solutions revealed an absence of phosphorus, thus indicating that no reaction had taken place. Due to the typically low solubility of phosphine gas in most organic solvents, very high pressures (ca. 30 atm) are often used.[97] In light of this, the reactions were repeated without nitrogen gas, that is, a phosphine base with 14 psi overpressure of phosphine. In this case, the stoichiometry could be controlled by careful observation of the measured overpressure; as phosphine reacts with the alkene it leaves the gaseous phase which in turn lowers the total pressure. As such, the reaction would reach stoichiometric completion when there is no more overpressure. However, NMR results of these reactions showed no phosphorus signal. In disregard for stoichiometry, the phosphine was increased to the maximum safe pressure (35 psi overpressure) for the apparatus. However, no phosphorus was found in the product. Interestingly, when this reaction was repeated using *t*-butylallylamine, the phosphorus NMR spectrum exhibited three peaks at -137, -68 and -30 ppm, which would correspond roughly to the primary, secondary, and tertiary phosphines, respectively. Unfortunately, subsequent attempts to reproduce these results were not successful.

In the final attempts at this pathway, a H_2 gas base with phosphine overpressure were used to mimic the mixture evolved from “fresh” phosphine production from elemental phosphorus in aqueous KOH solution which had been used in the

aforementioned synthesis of tris(thioether)phosphines. However this approach failed to produced any new alkylphosphines. In each reaction the solution exhibited a deep golden color upon heating which indicated the successful activation of the AIBN to its radical form. With the absence of product, it can be surmised that one of two things happened: either the AIBN radical did not react with PH_3 to make the phosphoryl radical, or the phosphoryl radical was made but did not react with the allyl amine. Due to the structure of the apparatus used and the inherently dangerous reactivity of PH_3, no techniques were available to probe the solution in order to confirm the presence of phosphoryl radicals.

Synthesis via Tri(alkynyl)phosphines

The next route attempted focused on the formation of tertiary phosphines via the copper-catalyzed coupling of PCl_3 with terminal alkynes (Scheme 2.6).

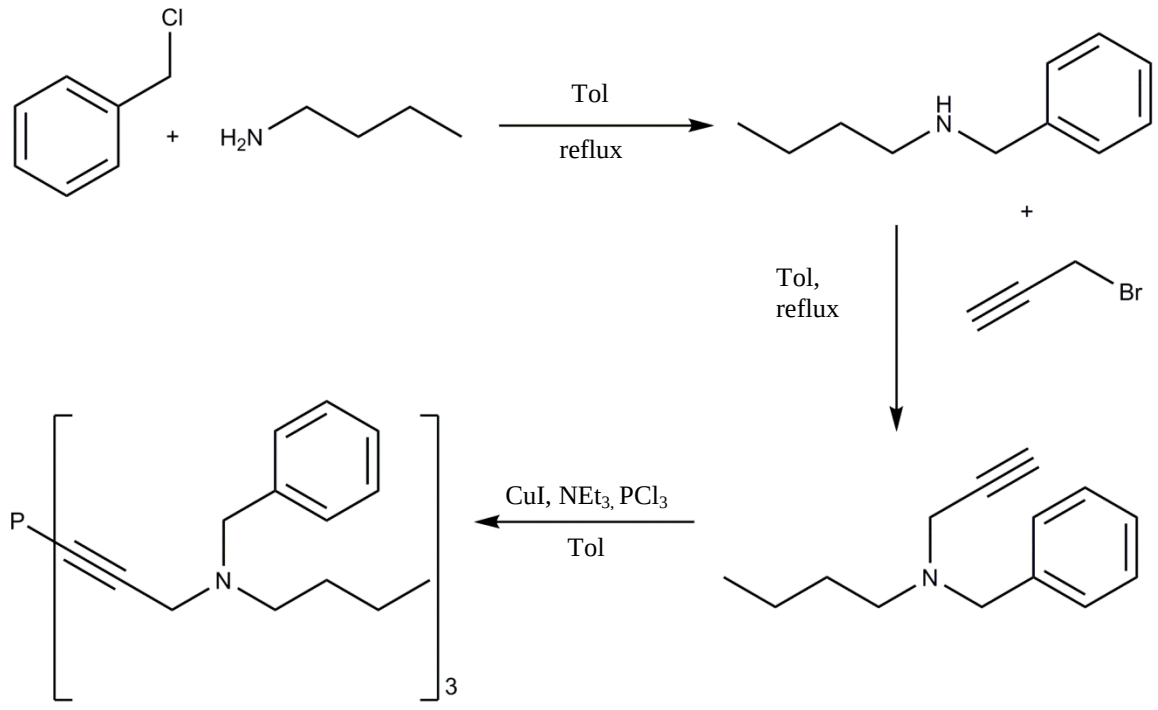

Scheme 2.6: Proposed route for the synthesis of tri(alkynyl)phosphines.

Afanasiev et al. were the first to report this method in which copper (I) iodide catalyzes the addition of terminal alkynes to chlorophosphines with the elimination of HCl.[98] In their proposed mechanism, the CuI functions in an identical fashion as in a Sonogashira reaction where the phosphine and alkyne coordinate in a cis position, followed by a base abstraction of the terminal alkynl proton in the elimination step. This study also reported the use of amine substituted alkynes but did not see any decline in conversion percentage. These tri(alkynyl)phosphines could then be used as is to form new phosphoniums, or they could possibly be hydrogenated to form more conventional trialkylphosphines. The Tolman electronic parameter for trivinylphosphine, $P(CH{=}{=}CH_2)_3$ is 2069.5 cm^{-1} which is similar to that of triphenylphosphine, 2068.9 cm^{-1}.[99] Likewise, a trialkynlphosphine could reasonably be expected to have electronic properties similar to both of those molecules. Tipically, triphenylphosphine creates phosphonium salts with inferior physical properties that are solids are room temperature; thus based on electronics alone, one might predict a trialkynylphosphine to produce similar results. If this were to happen, there would be several strategies that could be used to make this an attractive material, notably the idea of supported ionic liquids that are adsorbed onto silica or a polymer in a heterogenous system.[100]

In these attempts, there were a few successful productions of trialkynylphosphines. Unfortunately, however, no 100% reproducible results were obtained. The first problems were encountered in the synthesis of the tertiary alkynyl amines. The reaction of benzyl chloride with butylamine consistently performed as expected (around 60-70% yield). However, the following addition of propargyl bromide led to wide varying results. Some reactions led to the formation of the tertiary amine in moderate yields (50-65%) while others produced a black tar which solidified over time.

This product remained unchanged after addition of aqueous base indicating that it was not the ammonium salt. Additionally, proton and carbon NMR spectra of this product revealed no significant deviation from the desired liquid product. However, when this tar was used as a reagent, it was seen that no reaction occurred.

In the key copper catalyzed addition step, problems of reproducibility were encountered. Nevertheless, a few attempts successfully produced the desired trialkynylphosphine which displayed a ^{31}P signal at -90 ppm. This is well shifted from the expected peak of PCl_3 which would appear around +220 ppm if no reaction happened. In some other reactions, additional peaks appear around -40 and -45 ppm which may correspond to mono- and di-substituted chloroalkynylphosphines. In the attempts that did not produce any product, no precipitation of triethylammonium chloride was observed. This may be indicative of the needed acidity of the terminal alkynyl proton for this reaction to proceed. The trialkynylphosphine was successfully isolated, and a hydrogenation was attempted using Pd/C under hydrogen gas. However, under these conditions, no shift in the phosphorus spectrum was evident and the ^{13}C NMR revealed no additional peaks that would be expected upon the conversion of two quaternary carbons to sp^3 or sp^2 hybridization. Additionally, the loss of the benzyl substituent, which may have been in competition with the desired hydrogenation, was not observed.

Synthesis via Tetrakis(hydroxymethyl)phosphonium chloride

Following the two synthetic routes that were attempted, efforts were focused on molecules that already had existing P-C bonds that could therefore have amine functionalities added. The first such systems involves the precursor tetrakis(hydroxymethyl)phosphonium chloride. Under basic conditions, formaldehyde is eliminated and tris(hydroxylmethyl)phosphine is created (Scheme 2.7).

Tris(hydroxymethyl)phosphine has been shown to be a useful reagent for the creation of differently substituted phosphines.

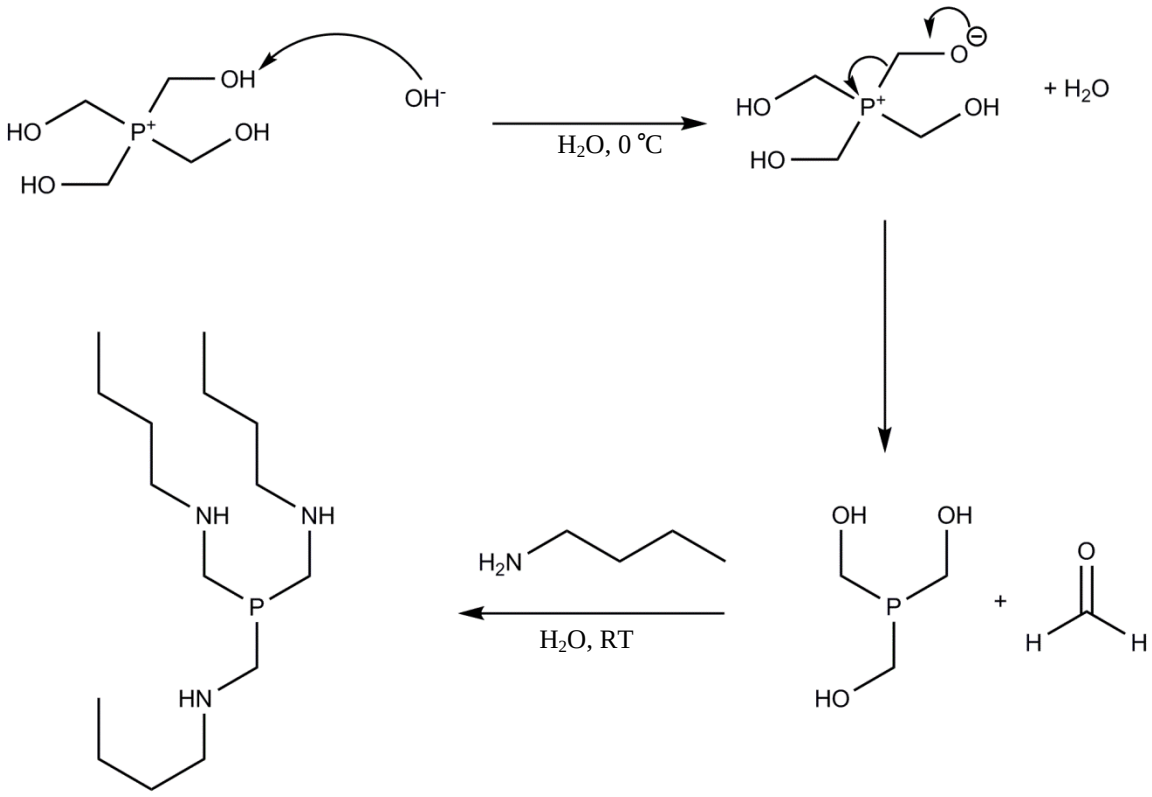

Scheme 2.7: Pathway for the synthesis of tri(aminomethyl)phosphines from tetrakis(hydroxymethyl)phosphonium salts.

The reactions displayed in Scheme 2.7 have been used extensively by Starosta et al. for the creation of multidentate aminomethylphosphines for coordination to copper (I) iodide.[101,102] Synthetically, it is often more advantageous to use the desired amine as the base in the elimination step so that the reaction can take place in a one-pot method. By use of this method, tris(butylaminomethyl)phosphine was synthesized in moderate yields (50-60%). This particular phosphine is an air-stable, light yellow oil at room temperature that is soluble in water and most polar organic solvents. The ^{31}P NMR spectrum had a

major peak at -63 ppm which corresponds well with signals reported for other tris(aminomethyl)phosphines.[101] Many low intensity signals were found randomly dispersed between -40 and -60 ppm and are probably due to small quantities of unknown impurities. To explore this further, a recrystallization from acetone was attempted in hope that this phosphine would produce the colorless crystals reported in the Starosta papers. However, no crystals were made and the oil was returned unaltered. While Starosta used more rigid morpholines and piperazines, the greater flexibility of straight chain alkyl groups could render crystallization disfavored. Interestingly, the oil did not solidify to a glass or a crystal when frozen at -40 ℃ for several days.

Subsequently, the phosphine was reacted with methyl iodide in acetonitrile, however, no clear sign of reaction was seen by NMR. Due to the unreactivity observed, a second pathway that would preserve the original phosphonium was developed (Scheme 2.8) from A. W. Frank's success in creating tris(aminomethyl)phosphine oxides.[103] In his work, the phosphonium was maintained by condensation of a weakly basic carbamate with tetrakis(hydroxymethyl)phosphonium chloride. After changing to a phosphine oxide, the carbamates were then cleaved to leave terminal amines as substituents. Using these results as a basis for further experimentation, tetrakis(hydroxymethyl)phosphonium chloride was reacted with 2-chloroacetamide to provide a linkage where butylamine could be added without loss of the phosphonium.

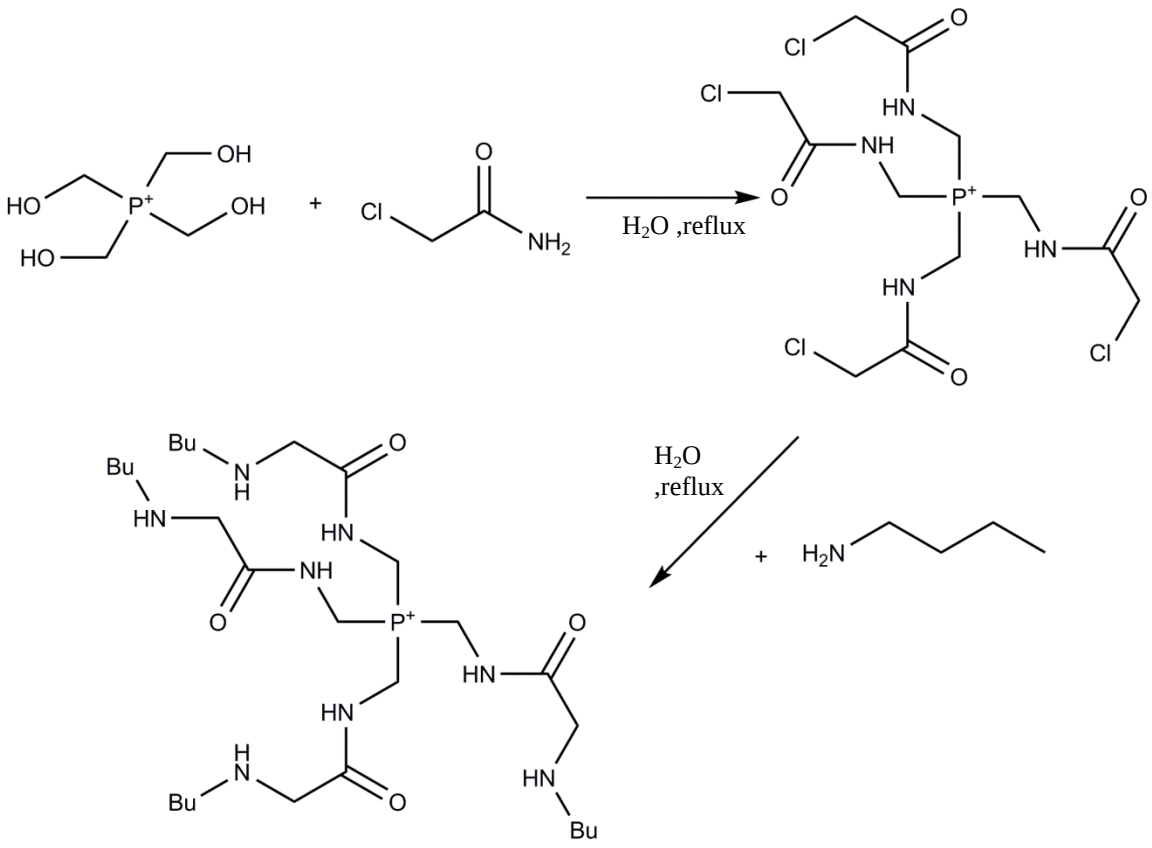

Scheme 2.8: Proposed route for the functionalization of tetrakis(hydroxymethyl)phosphonium chloride.

Unfortunately, the condensation reaction did not proceed to a measurable extent as evident from the ^{31}P NMR which showed no change from that of the tetrakis(hydroxymethyl)phosphonium chloride starting material. Additionally, proton and ^{13}C signals both indicated that unreacted tetrakis(hydroxymethyl)phosphonium chloride was the only species present. Acid catalyzed esterification was also attempted using 2-chloroacetic acid, however, this experiment also resulted in no reaction. This outcome may be due to the low nucleophilicity of the hydroxyls on the phosphonium substituents.

Synthesis via Ethanol Amines

The final pathway that was undertaken used di- and tri-ethanolamines as starting materials for the synthesis of ammonium ionic liquids with amine functionality (Scheme 2.9).

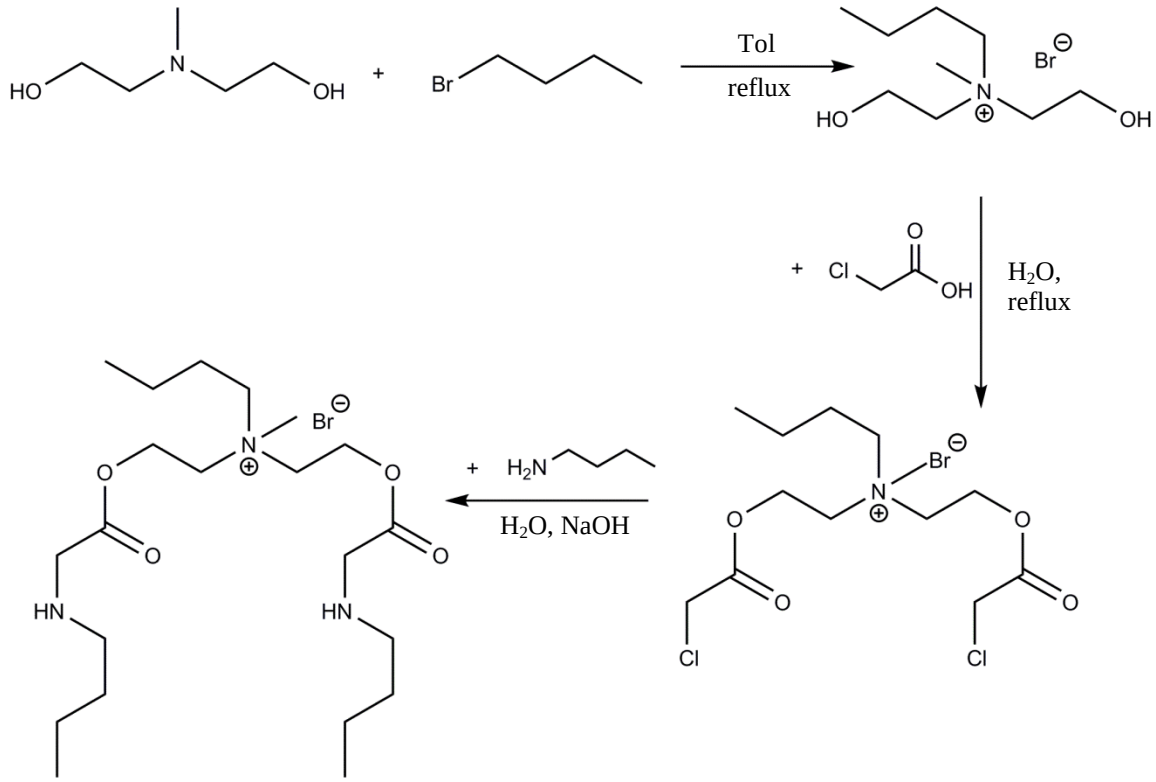

Scheme 2.9: Proposed synthetic pathway for the creation of new ammonium ionic liquids with attached amine functionalities.

In this process, di- or triethanolamine would be alkylated with a simple alkyl halide such a bromobutane creating the corresponding ethanolammonium salt. The hydroxyl groups on this salt could then undergo acid-catalyzed esterification with 2-chloroacetic acid to afford halides for SN2 reaction with butylamine. While these ammonium ionic liquids would not be able to have four amine substituents, they would

still be capable of at least 1:1 mol CO_2 absorption. Additionally, the ammonium cation based on triethanolamine would have three amines, which could present an interesting scenario in which the odd amine could either react intermolecularly with another cation or anion, or possibly not at all. In the synthesis, the alkylation of both diethanolmethylamine and triethanolamine proceeded very well, creating a viscous golden liquid at room temperature. This product was easily identified by the upfield shift that was apparent in the α protons adjoining the nitrogen atom. This product in and of itself represents and interesting entry into the library of ionic liquids. Typically, ammonium halides with this amount of alkyl chain length (i.e. tetrabutylammonium chloride) would be solids at room temperature. While there have been some instances of ionic liquids like this reported in the literature, they tend to be from the protonation of an ethanolamine with an organic acid and are not directly analogous.[104,105] Since the bromide salts alone have such favorable physical characteristics, ethanolammonium ionic liquids should be further investigated using BF_4, PF_6, of TFSI type anions to determine the effects on the physical properties. Unfortunately, when the ethanolammonium liquids were allowed to react with 2-chloroacetic acid in water, no product was formed. NMR studies of the resulting liquid showed both hydroxyl and acidic protons indicating that starting material had been returned. Thus, even though the ammonium center is two carbon atoms away, this may have affected the nucleophilicity of the hydroxyl moieties and decreased the chance of reaction.

Future Directions

The inconclusive results from the synthetic methods previously described leave many unanswered questions that merit thorough investigation. Unfortunately, time did not permit every possible avenue to be explored, leaving many pathways with options

that were not investigated. In the synthesis via PH_3, there are several procedural changes that could not in this work that may increase the chance of reaction. As an example, UV light could be used instead of a chemical to initiate radical formation in PH_3. Additionally, several of the successful systems reported previously utilized extreme pressures (~ 30 atm) or gas bubbling that could not be achieved in the available apparatus. Since the addition of allylamine to phosphine gas is a well known reaction,[106] there are probably some engineering issues that stand in the way of the addition of secondary allylamines.

In the two following pathways involving the synthesis of trialkynyl- and tris(aminomethyl)phosphines there are additional opportunities for further study. In addition to copper (I) iodide, terminal alkynes have also been shown to undergo similar couplings to PCl_3 using nickel and palladium catalysts.[107,108] Synthetically, it may also be easier to couple propargyl bromide and PCl_3 first before amination with butylamine. Based on the basicity of the alkynylphosphines observed in these studies, there may be a strong selectivity for an amine over the phosphine that would preclude formation of phosphoniums from homocoupling. When using tetrakis(hydroxylmethyl)phosphonium chloride, it might be interesting to try alkylating tris(hydroxymethyl)phosphine to see if a phosphonium is created under those conditions. This may indicate that the electronics of a β-amine may be factoring into the resistance of the tris(aminomethyl)phosphines to alkylation.

Finally, one interesting pathway using trivinylphosphine could be utilized. In 2003, Monkowius et al. prepared trivinylmethylphosphonium iodide from trivinylphosphine and methyl iodide. They found that quaternization greatly activated the reactivity of the vinyl substituents to reactions that would not occur in the parent phosphine.[109] Using this, they were able to achieve the addition of methanol across the

alkenes to create mono-, di-, and tris(methoxyethyl)methylphosphonium iodides. Since these vinyl groups are so susceptible to nucleophilic attack from alcohols, it may be possible to undergo hydroamination instead. In this case, a tris(alkylaminoethyl)methylphosphonium ionic liquid could be made with at least three amine functionalities. Alternately, an alcohol amine such as N-butyl, N-ethanolamine could be used to create phosphonium ILs with amines joined by flexible ether substituents.

CONCLUSIONS

Several different synthetic pathways were explored in efforts to prepare tetra-amine functionalized phosphonium and ammonium ionic liquids for the capture of carbon dioxide. Unfortunately, the original pathway developed produced both low yields and resulted in the formation of copious amounts of SO_2 and CO_2. Accordingly, a synthesis of aminophosphines was attempted through free radical addition to phosphine gas. In this, however, no free radical addition was detected despite the use of a variety of conditions. Following this, aminoalkynes were successfully coupled with PCl_3 by copper (I) iodide, however, no quaternization of these trialkynylphosphines was observed. In an effort to utilize existing P-C bonds, tetrakis(hydroxymethyl)phosphonium chloride was chosen as a reactant for the synthesis of a number of products. Tris(butylaminomethyl)phosphine was produced in good yield, but no phosphonium salts were produced when treated with various alkyl halides. Additionally, amide or ester linkers could not be added to the parent phosphonium under despite the use of a variety of conditions. Likewise, ester linkers could not be created on tri(ethanol)amine based ionic liquids, although the new ammonium salts created have interesting physical properties in and of themselves. While these avenues proved fruitless, several more possibilities exist that should be

investigated. Once the aforementioned synthetic problems are overcome, task-specific phosphonium and ammonium ionic liquids offer the promise of opening up new areas in ionic liquid research.

EXPERIMENTAL

General Considerations

All chemicals were purchased from Sigma-Aldrich Inc. All chemicals were of the highest available purity and used as received. All phosphine syntheses were performed under a dry, oxygen-free argon atmosphere or vacuum using standard Schlenk line and dry box techniques. All glassware was dried at least 24 h in a 120 °C oven prior to use. Toluene was distilled over sodium with a sodium benzophenone ketyl indicator and was degassed before use. Dichloromethane was distilled over calcium hydride.

Instrumentation

The NMR spectra were recorded on a Varian 300 Unity Plus spectrometer (300 MHz, 298K). For ^{1}H and ^{13}C spectra, chemical shifts are referenced to the deuterated solvent while CHF_3 and H_3PO_4 were used for ^{19}F and ^{31}P, respectively

Synthesis

N-butyl, N-(2-chloroethyl)ammonium chloride

5.0 g of N-butyl, N-ethanolamine was added to 20 ml of THF and chilled in an ice bath. Approximately 5 grams of thionyl chloride was slowly added dropwise to the stirred solution over the course of an hour and allowed to warm to room temperature over another hour. Excess $SOCl_2$ was neutralized with water, and the resulting ammonium precipitate was filtered and dried under vacuum. Yield: 5.51 g (74%) ^{1}H ($CDCl_3$, ppm) δ:

0.91 (m, 3H, CH_3), 1.35 (m, 2H, CH_3CH_2), 1.77 (m, 2H, $CH_3CH_2CH_2$), 2.90 (m, 2H, CH_2Cl), 3.23 (m, 2H, CH_2N), 3.89 (m, 2H, NCH_2CH_2Cl), 9.45, (s, 2H, NH_2^+)

N-butyl, N-allylamine

10 g of butylamine and a slight deficit of 15 g allyl bromide were added to 50 ml of toluene in a round bottom flask. The solution was stirred and lightly refluxed overnight. The resulting ammonium precipitate was filtered and washed with hexanes. If used as the ammonium salt, the solid was dried before use, otherwise it was dissolved in water. 1M NaOH was then added until the solution had a pH 11 or higher, and the amine was extracted several times with diethylether. This extract was then distilled to remove residual butylamine. Yield: 9.68 g (62%) ^1H ($CDCl_3$, ppm) δ: 0.81 (m, 3H, CH_3), 1.07-1.39 (m, 4H, $CH_3CH_2CH_2$), 2.49 (m, 2H, CH_2CH_2N), 3.13 (m, 2H, $NCH_2CH{=}CH_2$), 4.95 (m, 2H, $CH{=}CH_2$), 5.78 (m, 1H, $CH{=}CH_2$) $^{13}C\{^1H\}$ ($CDCl_3$, ppm) δ: 13.7 (CH_3), 20.23 (CH_3CH_2), 31.9 ($CH_3CH_2CH_2$), 48.8 (CH_2N), 52.6 ($NCH_2CH{=}CH_2$), 115.4 ($CH{=}CH_2$), 136.6 ($CH{=}CH_2$)

N-t-butyl, N-allylamine

10 g of t-butylamine and a slight deficit of 15 g allyl bromide were added to 50 ml of toluene in a round bottom flask. The solution was stirred and lightly refluxed overnight. The resulting ammonium precipitate was filtered and washed with hexanes and dissolved in water. 1M NaOH was then added until the solution had a pH 11 or higher, and the amine was extracted several times with diethylether. This extract was then distilled to remove residual t-butylamine. Yield: 8.57 g (55%) ^1H ($CDCl_3$, ppm) δ: 1.05 (m, 9H, CH_3), 2.56 (m, 2H, $NCH_2CH{=}CH_2$), 4.95 (m, 2H, $CH{=}CH_2$), 5.78 (m, 1H,

$CH=CH_2$) $^{13}C\{^1H\}$ ($CDCl_3$, ppm) δ: 28.8 (CH_3), 49.8 ($NCH_2CH=CH_2$), 116.1 ($CH=CH_2$), 136.4 ($CH=CH_2$)

Free radical addition general procedure

14.4 g of butylallylamine or 24.7 g of the corresponding ammonium bromides were dissolved in 100 ml of acetonitrile. Approximately 100 mg of AIBN and a stir bar was added and the solution was thoroughly degassed with argon before being added to a sealed 1 L reaction vessel in a dry box. This reaction vessel was then degassed with nitrogen before being charged with phosphine gas (usually 14 psi overpressure). The vessel was sealed and heated until the solution formed a bright golden color whereupon the temperature was held constant for several hours. Afterwards, the vessel was degassed by argon into a $CuSO_4$ solution for safe PH_3 disposal and NMR samples were taken in the dry box. NMR samples typically consisted of one part solution to four parts CD_3CN.

N-benzyl, N-butylamine

10g of butylamine and approximately 17 g of benzyl chloride were combined in 50 ml of toluene and refluxed overnight. The resulting ammonium precipitate was filtered and washed with hexanes and dissolved in water. 1M NaOH was then added until the solution had a pH 11 or higher, and the amine was extracted several times with diethylether. This extract was then distilled to remove residual butylamine. Yield: 15.17 g (68%) ^1H ($CDCl_3$, ppm) δ: 0.81 (m, 3H, CH_3), 1.07-1.39 (m, 4H, $CH_3CH_2CH_2$), 2.49 (m, 2H, CH_2CH_2N), 3.13 (m, 2H, NCH_2Ar), 7.21-7.59 (m, 5H, Ar) $^{13}C\{^1H\}$ ($CDCl_3$, ppm) δ: 13.7 (CH_3), 20.23 (CH_3CH_2), 27.9 ($CH_3CH_2CH_2$), 46.1 (CH_2N), 50.7 (NCH_2Ph), 127.2, 127.5, 128.65, 129.2, 129.5 (Ar)

N-benzyl, N-butyl, propynylamine

5 g of N-benzyl, N-butylamine was combined with approximately 3.5 g of propargyl bromide in 25 ml of toluene. The solution was very lightly refluxed overnight. The resulting ammonium precipitate was filtered and washed with hexanes and dissolved in water. 1M NaOH was then added until the solution had a pH 11 or higher, and the amine was extracted several times with diethylether. Yield: 3.38 g (54%) ^{1}H ($CDCl_3$, ppm) δ: 0.85 (m, 3H, CH_3), 1.25 (m, 2H, $CH_3CH_2CH_2$), 1.87 (m, 2H, $CH_3CH_2CH_2$), 2.84 (m, 2H, CH_2CH_2N), 3.13 (m, 2H, NCH_2Ar), 3.51 (s, 1H, CH), 3.78 (d, 2H, CH_2), 7.31-7.59 (m, 5H, Ar) $^{13}C\{^{1}H\}$ ($CDCl_3$, ppm) δ: 14.5 (CH_3), 20.9 (CH_3CH_2), 30.1 ($CH_3CH_2CH_2$), 41.7 (alkynyl CH_2N), 45.5 (CH_2N), 58.5 (NCH_2Ph), 73.5 (CH), 79.1 (C), 127.2, 127.5, 128.65, 129.2, 129.5 (Ar)

Tris(3-(N-benzyl, N-butylamino)propynyl)phosphine

3 g of N-benzyl, N-butyl, propynylamine and 3 g of triethylamine were dissolved in 25 ml of toluene and degassed with argon. In a dry box, 10 mol % was added to this solution. Following that, 0.60 g of PCl_3 in 10 ml toluene was added dropwise over several hours. The solution was allowed to stir overnight under inert atmosphere and was filtered through a Schlenk frit. To the filtrate, 10 ml degassed water was slowly added at 0 ℃. The organic layer was extracted and dried under vacuum to yield a dark liquid. Yield: 3.04 g (89%) ^{1}H ($CDCl_3$, ppm) δ: 0.75 (m, 3H, CH_3), 1.10-1.39 (m, 4H, $CH_3CH_2CH_2$), 2.44 (m, 2H, CH_2CH_2N), 3.13 (m, 2H, NCH_2Ar), 3.78 (d, 2H, CH_2), 7.31-7.59 (m, 5H, Ar) $^{13}C\{^{1}H\}$ ($CDCl_3$, ppm) δ: 15.5 (CH_3), 20.9 (CH_3CH_2), 29.7 ($CH_3CH_2CH_2$), 41.5

(alkynyl CH_2N), 53.7 (CH_2N), 58.3 (NCH_2Ph), 77.1 (C), 127.2, 127.5, 128.65, 129.2, 129.5 (Ar) ^{31}P ($CDCl_3$, ppm) δ: -89.5

Tris(butylaminomethyl)phosphine

10 g of tetrakis(hydroxymetyl)phosphonium chloride (80 wt % in H_2O) was added to 10 ml of water and degassed. Under inert atmosphere, 12.5 g of butylamine was added dropwise over several hours. The aqueous solution was extracted with chloroform and the organic layer was stripped of solvent under vacuum giving a deep yellow oil. Yield: 7.27 g, (60%) ^{1}H ($CDCl_3$, ppm) δ: 0.75 (m, 3H, CH_3), 0.67 (m , 9H, CH_3), 1.05-1.30 (m, 12H, $CH_3CH_2CH_2$), 2.05-2.45 (m, 12H, NCH_2), 2.60 (m, 3H, NH) $^{13}C\{^{1}H\}$ ($CDCl_3$, ppm) δ: 14.2 (CH_3), 20.6 (CH_3CH_2), 29.5 ($CH_3CH_2CH_2$), 50.4 (NCH_2), 57.3 (PCH_2) ^{31}P ($CDCl_3$, ppm) δ: --63.9

Bis(2-hydroxyethyl)methylpentylammonium bromide

In 25 ml tolueme, 10 g of di(ethanol)methylamine and 11.5 g of bromopentane were combined and refluxed overnight. In the resulting biphasic system, the top toluene layer was extracted and the bottom layer was washed several times with hexane and ethyl acetate. The layer was then dried under vacuum for several hours to afford the ammonium salt as a deep golden liquid. Yield: 14.2 g (66%) ^{1}H (CD_3OD, ppm) δ: 1.01 (m, 3H, CH_3), 1.40 (m, 2H, CH_3CH_2), 1.82 (m, 2H, $CH_3CH_2CH_2$), 3.25 (s, 3H, NCH_3), 3.51-3.69 (m, 6H, NCH_2), 4.05 (m, 4H, $HOCH_2$), 4.51 (s, 2H, OH) $^{13}C\{^{1}H\}$ (CD_3OD, ppm) δ:12.8 (CH_3), 19.6 (CH_3CH_2), 24.3 ($CH_3CH_2CH_2$), 49.3 (NCH_3), 55.6 (NCH_2), 63.8 (d, $HOCH_2$)

REFERENCES

(1) Broeke, J. Van Den; Deelman, B.; Koten, G. Van. *Tetrahedron Lett.* **2001**, *42*, 8085–8087.

(2) Bulut, S.; Klose, P.; Huang, M.-M.; Weingärtner, H.; Dyson, P. J.; Laurenczy, G.; Friedrich, C.; Menz, J.; Kümmerer, K.; Krossing, I. *Chemistry* **2010**, *16*, 13139–13154.

(3) Ignat'ev, N. V.; Welz-Biermann, U.; Kucheryna, A.; Bissky, G.; Willner, H. *J. Fluor. Chem.* **2005**, *126*, 1150–1159.

(4) MacFarlane, D. R.; Forsyth, S. a.; Golding, J.; Deacon, G. B. *Green Chem.* **2002**, *4*, 444–448.

(5) Tsunashima, K.; Sugiya, M. *Electrochemistry Communications*, 2007, *9*, 2353–2358.

(6) Tsunashima, K.; Sugiya, M. *Electrochemistry* **2007**, *75*, 734–736.

(7) Del Sesto, R. E.; Corley, C.; Robertson, A.; Wilkes, J. S. *J. Organomet. Chem.* **2005**, *690*, 2536–2542.

(8) Armel, V.; Velayutham, D.; Sun, J.; Howlett, P. C.; Forsyth, M.; Macfarlane, D. R.; Pringle, J. M. *J. Mater. Chem.* **2011**, 7640–7650.

(9) Erdmenger, T.; Vitz, J.; Wiesbrock, F.; Schubert, U. S. *J. Mater. Chem.* **2008**, *18*, 5267.

(10) Pinal, R. *Org. Biomol. Chem.* **2004**, *2*, 2692–2699.

(11) Han, H.; Liu, K.; Feng, S.; Zhou, S.; Feng, W.; Nie, J.; Li, H.; Huang, X.; Matsumoto, H.; Armand, M.; Zhou, Z. *Electrochim. Acta* **2010**, *55*, 7134–7144.

(12) Katsyuba, S. A.; Zvereva, E. E.; Vidis, A.; Dyson, P. J. *J. Phys. Chem. A* **2007**, *111*, 352–370.

(13) Trohalaki, S.; Pachter, R.; Drake, G. W.; Hawkins, T. *Energy & Fuels* **2005**, *19*, 279–284.

(14) Krossing, I.; Slattery, J. *J. Am. Chem. Soc.* **2006**, 13427–13434.

(15) Yella, A.; Lee, H.-W.; Tsao, H. N.; Yi, C.; Chandiran, A. K.; Nazeeruddin, M. K.; Diau, E. W.-G.; Yeh, C.-Y.; Zakeeruddin, S. M.; Grätzel, M. *Science* **2011**, *334*, 629–634.

(16) Sargent, E. H. *Nat. Photonics* **2012**, *6*, 133–135.

(17) Kaltenbrunner, M.; White, M. S.; Głowacki, E. D.; Sekitani, T.; Someya, T.; Sariciftci, N. S.; Bauer, S. *Nat. Commun.* **2012**, *3*, 770.

(18) Battaglia, C.; Escarré, J.; Söderström, K.; Charrière, M.; Despeisse, M.; Haug, F.-J.; Ballif, C. *Nat. Photonics* **2011**, *5*, 535–538.

(19) Klahr, B. M.; Martinson, A. B. F.; Hamann, T. W. *Langmuir* **2011**, *27*, 461–468.

(20) Lee, K.; Ahn, B. T.; Son, C.-S.; Su, C.-Y.; Ho, W.-H.; Lin, H.-C.; Nieh, C.-Y.; Liang, S.-C. *Sol. Energy Mater. Sol. Cells* **2011**, *95*, 261–263.

(21) Brendel, R. *Thin-Film Crystalline Silicon Solar Cells: Physics and Technology (Google eBook)*; John Wiley & Sons, 2011; p. 306.

(22) Wang, S.; Swingle, S. F.; Ye, H.; Fan, F.-R. F.; Cowley, A. H.; Bard, A. J. *J. Am. Chem. Soc.* **2012**, *134*, 11056–11059.

(23) Green, M. A.; Emery, K.; Hishikawa, Y.; Warta, W.; Dunlop, E. D. *Prog. Photovoltaics Res. Appl.* **2012**, *20*, 12–20.

(24) Dupret, F.; Derby, J. J.; Kakimoto, K.; Müller, G.; Van den Bogaert, N.; Wheeler, A. A.; Dornberger, E.; Tomzig, E.; Seidl, A.; Schmitt, S.; Leister, H.-J.; Schmitt, C. *J. Cryst. Growth* **1997**, *180*, 461–467.

(25) Braga, A. F. B.; Moreira, S. P.; Zampieri, P. R.; Bacchin, J. M. G.; Mei, P. R. *Sol. Energy Mater. Sol. Cells* **2008**, *92*, 418–424.

(26) S. Benagli, D. Borrello, E. Vallat-Sauvain, Meier J, Kroll U, Hötzel J, Spitznagel J, Steinhauser J, Castens L, D. Y. In *24th European Photovoltaic Solar Energy Conference,*; 2009.

(27) Yamamoto K, Toshimi M, Suzuki T, Tawada Y, Okamoto T, N. A. In *MRS Spring Meeting*; 1998.

(28) Chopra, K. L.; Paulson, P. D.; Dutta, V. *Prog. Photovoltaics Res. Appl.* **2004**, *12*, 69–92.

(29) Bard, Allen J, Faulkner, L. R. *Electrochemical Methods: Fundamentals and Applications*; 2nd ed.; John Wiley & Sons: Danvers, 2001; p. 887.

(30) S. P. Shavkunov, T. L. S. *Russ. J. Electrochem.* **2003**, *39*, 642 – 649.

(31) Bittolo Bon, S.; Valentini, L.; Kenny, J. M.; Peponi, L.; Verdejo, R.; Lopez-Manchado, M. a. *Phys. Status Solidi* **2010**, *207*, 2461–2466.

(32) Saitou, M.; Sakae, K.; Oshikawa, W. *Surf. Coatings Technol.* **2003**, *162*, 101–105.

(33) Agrawal, A. K. *J. Electrochem. Soc.* **1981**, *128*, 2292.

(34) Osaka, T.; Saboungi, M.-L.; Selman, J. R.; Fukunaka, Y.; Nishimura, Y.; Fukunaka, Y. *Electrochim. Acta* **2007**, *53*, 111–116.

(35) Munisamy, T.; Bard, A. J. *Electrochim. Acta* **2010**, *55*, 3797–3803.

(36) Bechelany, M.; Elias, J.; Brodard, P.; Michler, J.; Philippe, L. *Thin Solid Films* **2012**, *520*, 1895–1901.

(37) Simka, W.; Puszczyk, D.; Nawrat, G. *Electrochim. Acta* **2009**, *54*, 5307–5319.

(38) NuLi, Y.; Yang, J.; Wang, P. *Appl. Surf. Sci.* **2006**, *252*, 8086–8090.

(39) Endres, F.; El Abedin, S. Z. *Chem. Commun.* **2002**, 892–893.

(40) Endres, F.; Zein El Abedin, S. *Phys. Chem. Chem. Phys.* **2002**, *4*, 1649–1657.

(41) Abedin, S. Z. El; Borissenko, N.; Endres, F. *Electrochem. commun.* **2004**, *6*, 510–514.

(42) Al-Salman, R.; Meng, X.; Zhao, J.; Li, Y.; Kynast, U.; Lezhnina, M. M.; Endres, F. *Pure Appl. Chem.* **2010**, *82*, 1673–1689.

(43) Lahiri, A.; Willert, A.; Abedin, S. Z. El; Endres, F. *Electrochim. Acta* **2014**, *121*, 154–158.

(44) Meng, X.; Al-Salman, R.; Zhao, J.; Borissenko, N.; Li, Y.; Endres, F. *Angew. Chem. Int. Ed. Engl.* **2009**, *48*, 2703–2707.

(45) Endres, F.; Höfft, O. *Phys. Chem. Chem. Phys.* **2010**, *12*, 1724–1732.

(46) Pulletikurthi, G.; Lahiri, A.; Carstens, T.; Borisenko, N.; Zein El Abedin, S.; Endres, F. *J. Solid State Electrochem.* **2013**, *17*, 2823–2832.

(47) Tsunashima, K.; Niwa, E. *J. Phys. Chem. B* **2009**, *113*, 15870–15874.

(48) Tindale, J.; Ragogna, P. *Chem. Commun.* **2009**, 1831–1833.

(49) Ahrens, S.; Peritz, A.; Strassner, T. *Angew. Chem. Int. Ed. Engl.* **2009**, *48*, 7908–7910.

(50) Jin, H.; O'Hare, B.; Dong, J.; Arzhantsev, S.; Baker, G. A.; Wishart, J. F.; Benesi, A. J.; Maroncelli, M. *J. Phys. Chem. B* **2008**, *112*, 81–92.

(51) Xu, W.; Cooper, E. I.; Angell, C. A. *J. Phys. Chem. B* **2003**, *107*, 6170–6178.

(52) Buzzeo, M. C.; Evans, R. G.; Compton, R. G. *Chemphyschem* **2004**, *5*, 1106–1120.

(53) Gobet, J. *J. Electrochem. Soc.* **1988**, *135*, 109.

(54) Borisenko, N.; Zein El Abedin, S.; Endres, F. *J. Phys. Chem. B* **2006**, *110*, 6250–6256.

(55) Nishimura, Y.; Fukunaka, Y.; Nishida, T.; Nohira, T.; Hagiwara, R. *Electrochem. Solid-State Lett.* **2008**, *11*, D75.

(56) Cole, A. C.; Jensen, J. L.; Ntai, I.; Tran, K. L. T.; Weaver, K. J.; Forbes, D. C.; Davis, J. H. *J. Am. Chem. Soc.* **2002**, *124*, 5962–5963.

(57) Yue, C.; Mao, A.; Wei, Y.; Lü, M. *Catal. Commun.* **2008**, *9*, 1571–1574.

(58) Anthony, J. L.; Maginn, E. J.; Brennecke, J. F. *J. Phys. Chem. B* **2002**, *106*, 7315–7320.

(59) Tempel, D. J.; Henderson, P. B.; Brzozowski, J. R.; Pearlstein, R. M.; Cheng, H. *J. Am. Chem. Soc.* **2008**, *130*, 400–401.

(60) Barnea, Z.; Sachs, T.; Chidambaram, M.; Sasson, Y. *J. Hazard. Mater.* **2013**, *244-245*, 495–500.

(61) Huang, K.; Cai, D.-N.; Chen, Y.-L.; Wu, Y.-T.; Hu, X.-B.; Zhang, Z.-B. *Chem. Eng. J.* **2013**, *59*, 2227–2235.

(62) Wu, W.; Han, B.; Gao, H.; Liu, Z.; Jiang, T.; Huang, J. *Angew. Chem. Int. Ed. Engl.* **2004**, *43*, 2415–2417.

(63) Huang, K.; Chen, Y.-L.; Zhang, X.-M.; Xia, S.; Wu, Y.-T.; Hu, X.-B. *Chem. Eng. J.* **2014**, *237*, 478–486.

(64) Huang, K.; Wang, G.-N.; Dai, Y.; Wu, Y.-T.; Hu, X.-B.; Zhang, Z.-B. *RSC Adv.* **2013**, *3*, 16264.

(65) Qu, G.; Zhang, J.; Li, J.; Ning, P. *Sep. Sci. Technol.* **2013**, *48*, 2876–2879.

(66) Palomar, J.; Gonzalez-Miquel, M.; Bedia, J.; Rodriguez, F.; Rodriguez, J. J. *Sep. Purif. Technol.* **2011**, *82*, 43–52.

(67) Le Quéré, C.; Peters, G. P.; Andres, R. J.; Andrew, R. M.; Boden, T.; Ciais, P.; Friedlingstein, P.; Houghton, R. A.; Marland, G.; Moriarty, R.; Sitch, S.; Tans, P.; Arneth, A.; Arvanitis, A.; Bakker, D. C. E.; Bopp, L.; Canadell, J. G.; Chini, L. P.; Doney, S. C.; Harper, A.; Harris, I.; House, J. I.; Jain, A. K.; Jones, S. D.; Kato, E.; Keeling, R. F.; Klein Goldewijk, K.; Körtzinger, A.; Koven, C.; Lefèvre, N.; Omar, A.; Ono, T.; Park, G.-H.; Pfeil, B.; Poulter, B.; Raupach, M. R.; Regnier, P.; Rödenbeck, C.; Saito, S.; Schwinger, J.; Segschneider, J.; Stocker, B. D.; Tilbrook, B.; van Heuven, S.; Viovy, N.; Wanninkhof, R.; Wiltshire, A.; Zaehle, S.; Yue, C. *Earth Syst. Sci. Data Discuss.* **2013**, *6*, 689–760.

(68) Rochelle, G. T. *Science* **2009**, *325*, 1652–1654.

(69) Choi, S.; Drese, J. H.; Jones, C. W. *ChemSusChem* **2009**, *2*, 796–854.

(70) Abanades, J. C.; Alvarez, D. *Energy & Fuels* **2003**, *17*, 308–315.

(71) Michelena, J. A.; Peeters, G.; Vansant, E. F.; de Bièvre, P. *Recl. des Trav. Chim. des Pays-Bas* **2010**, *96*, 121–124.

(72) Harlick, P. J. E.; Sayari, A. *Ind. Eng. Chem. Res.* **2006**, *45*, 3248–3255.

(73) Eddaoudi, M.; Kim, J.; Rosi, N.; Vodak, D.; Wachter, J.; O'Keeffe, M.; Yaghi, O. M. *Science* **2002**, *295*, 469–472.

(74) Llewellyn, P. L.; Bourrelly, S.; Serre, C.; Vimont, A.; Daturi, M.; Hamon, L.; De Weireld, G.; Chang, J.-S.; Hong, D.-Y.; Kyu Hwang, Y.; Hwa Jhung, S.; Férey, G. *Langmuir* **2008**, *24*, 7245–7250.

(75) Comotti, A.; Bracco, S.; Sozzani, P.; Horike, S.; Matsuda, R.; Chen, J.; Takata, M.; Kubota, Y.; Kitagawa, S. *J. Am. Chem. Soc.* **2008**, *130*, 13664–13672.

(76) Arstad, B.; Fjellvåg, H.; Kongshaug, K. O.; Swang, O.; Blom, R. *Adsorption* **2008**, *14*, 755–762.

(77) Dietzel, P. D. C.; Besikiotis, V.; Blom, R. *J. Mater. Chem.* **2009**, *19*, 7362.

(78) Caskey, S. R.; Wong-Foy, A. G.; Matzger, A. J. *J. Am. Chem. Soc.* **2008**, *130*, 10870–10871.

(79) McDonald, T. M.; D'Alessandro, D. M.; Krishna, R.; Long, J. R. *Chem. Sci.* **2011**, *2*, 2022.

(80) Sumida, K.; Rogow, D. L.; Mason, J. a; McDonald, T. M.; Bloch, E. D.; Herm, Z. R.; Bae, T.-H.; Long, J. R. *Chem. Rev.* **2012**, *112*, 724–781.

(81) Ramdin, M.; de Loos, T. W.; Vlugt, T. J. H. *Ind. Eng. Chem. Res.* **2012**, *51*, 8149–8177.

(82) Aki, S. N. V. K.; Mellein, B. R.; Saurer, E. M.; Brennecke, J. F. *J. Phys. Chem. B* **2004**, *108*, 20355–20365.

(83) Bates, E. D.; Mayton, R. D.; Ntai, I.; Davis, J. H. *J. Am. Chem. Soc.* **2002**, *124*, 926–927.

(84) Gutowski, K. E.; Maginn, E. J. *J. Am. Chem. Soc.* **2008**, *130*, 14690–14704.

(85) Zhang, J.; Jia, C.; Dong, H.; Wang, J.; Zhang, X.; Zhang, S. *Ind. Eng. Chem. Res.* **2013**, *52*, 5835–5841.

(86) Zhang, Y.; Zhang, S.; Lu, X. *Chem. Eur. J.* **2009**, *15*, 3003–3011.

(87) Xue, Z.; Zhang, Z.; Han, J.; Chen, Y.; Mu, T. *Int. J. Greenh. Gas Control* **2011**, *5*, 628–633.

(88) Wang, C.; Cui, G.; Luo, X.; Xu, Y.; Li, H.; Dai, S. *J. Am. Chem. Soc.* **2011**, *133*, 11916–11919.

(89) Tang, H.; Wu, C. *ChemSusChem* **2013**, *6*, 1050–1056.

(90) Goodrich, B.; Fuente, J. de la. *Ind. Eng. Chem. Res.* **2010**, *50*, 111–118.

(91) Goodrich, B. F.; de la Fuente, J. C.; Gurkan, B. E.; Lopez, Z. K.; Price, E. A.; Huang, Y.; Brennecke, J. F. *J. Phys. Chem. B* **2011**, *115*, 9140–9150.

(92) Feng, Z.; Cheng-Gang, F.; You-Ting, W.; Yuan-Tao, W.; Ai-Min, L.; Zhi-Bing, Z. *Chem. Eng. J.* **2010**, *160*, 691–697.

(93) Zhao, Y.; Zhang, X.; Zeng, S.; Zhou, Q.; Dong, H.; Tian, X.; Zhang, S. *J. Chem. Eng. Data* **2010**, *55*, 3513–3519.

(94) Zhang, X.; Dong, H.; Zhao, Z. *Energy Environ. Sci.* **2012**, *5*, 6668–6681.

(95) Rauhut, M. M.; Currier, H. A.; Semsel, A. M.; Wystratch, V. P. *J. Org. Chem.* **1961**, *26*, 5138–5145.

(96) Gusarova, N. K.; Ivanova, N. I.; Bogdanova, M. V; Sinegovskaya, L. M.; Gusarov, A. V; Trofimov, B. A. *Phosphorus, Sulfur, and Silicon* **2005**, 1749–1754.

(97) Trofimov, B.; Arbuzova, S.; Gusarova, N. *Russ. Chem. Rev.* **1999**, *68*, 215–227.

(98) Afanasiev, V. V.; Beletskaya, I. P.; Kazankova, M. a.; Efimova, I. V.; Antipin, M. U. *Synthesis (Stuttg).* **2003**, 2835–2838.

(99) Tolman, C. *Chem. Rev.* **1977**, *1976*, 313.

(100) *Supported Ionic Liquids: Fundamentals and Applications (Google eBook)*; John Wiley & Sons, 2013; p. 400.

(101) Starosta, R.; Florek, M.; Król, J. *New J. Chem.* **2010**, *34*, 1441.

(102) Starosta, R.; Komarnicka, U. K.; Puchalska, M.; Barys, M. *New J. Chem.* **2012**, *36*, 1673.

(103) Frank, A. *Can. J. Chem.* **1981**, 1–7.

(104) Petrović, Z. D.; Marković, S.; Petrović, V. P.; Simijonović, D. *J. Mol. Model.* **2012**, *18*, 433–440.

(105) Pinkert, A.; Ang, K. L.; Marsh, K. N.; Pang, S. *Phys. Chem. Chem. Phys.* **2011**, *13*, 5136–5143.

(106) Stiles, A. R.; Rust, F. F.; Vaughan, W. E. *J. Am. Chem. Soc.* **1952**, *74*, 3282–3284.

(107) Ochida, A.; Sawamura, M. *Chem. Asian J.* **2007**, *2*, 609–618.

(108) Beletskaya, I. P.; Afanasiev, V. V; Kazankova, M. A.; Efimova, I. V. *Org. Lett.* **2003**, *5*, 4309–4311.

(109) Monkowius, U.; Nogai, S.; Schmidbaur, H. *Organometallics* **2003**, 145–152.